Downloaded from orbit.dtu.dk on: Apr 26, 2024

DTU Library

# Balancing Tool Chain: Balancing and automatic control in North Sea Countries in 2020, 2030 and 2050

**Kanellas, Polyneikis; Das, Kaushik; Gea-Bermudez, Juan; Sørensen, Poul**

*Publication date:*
2020

*Document Version*
Publisher's PDF, also known as Version of record

Link back to DTU Orbit

*Citation (APA):*
Kanellas, P., Das, K., Gea-Bermudez, J., & Sørensen, P. (2020). *Balancing Tool Chain: Balancing and automatic control in North Sea Countries in 2020, 2030 and 2050*. DTU Wind Energy. DTU Wind Energy E Vol. 0199

**General rights**
Copyright and moral rights for the publications made accessible in the public portal are retained by the authors and/or other copyright owners and it is a condition of accessing publications that users recognise and abide by the legal requirements associated with these rights.

- Users may download and print one copy of any publication from the public portal for the purpose of private study or research.
- You may not further distribute the material or use it for any profit-making activity or commercial gain
- You may freely distribute the URL identifying the publication in the public portal

If you believe that this document breaches copyright please contact us providing details, and we will remove access to the work immediately and investigate your claim.

# Balancing Tool Chain : Balancing and automatic control in North Sea Countries in 2020, 2030 and 2050

Department of Wind Energy

E Report 2020

NSON-DK

Deliverable 3.2


Polyneikis Kanellas, DTU Wind Energy

Kaushik Das, DTU Wind Energy

Juan Gea-Bermúdez, DTU Management

Poul Sørensen, DTU Wind Energy



DTU Wind Energy E-0199

Mar 2020



DTU Wind Energy
Department of Wind Energy

DTU Management Engineering
Department of Management Engineering

**Authors:** Polyneikis Kanellas[1], Kaushik Das[1], Juan Gea-Bermúdez[2] and Poul Sørensen[1]

**Title:** Balancing Tool Chain : Balancing and automatic control in North Sea Countries in 2020, 2030 and 2050

**Department:** [1]DTU Wind Energy. [2]DTU Management

**DTU Wind Energy E-0199**

**Mar 2020**

**Summary:**

This report analyses a study in the balancing operation of the power system of North Sea countries with focus on the Danish power system and its regions DK1 and DK2. The study covers all the steps of the operation from the Day Ahead Market to the Real Time balancing of generation and demand. For that reason, a balancing tool chain has been developed.

The report analyses a) the value of offshore grid on balancing of forecast errors, b) the impact of forecast errors on manual and automatic reserves and c) the quality of electrical frequency in the near future considering high VRE penetration.

The simulation results clearly shows that the offshore grid scenario has very similar impact on balancing of reserves to project based scenario. Since offshore grid scenario provides additional values like increased security and flexibility as well as larger integration of North Sea countries, having similar impact on balancing as that of project based, makes offshore grid a recommendable option for future grid development. Additionally, real-time imbalance in Nordic network is much lower in case of Offshore grid scenario as compared to Project based scenario.

Day ahead market simulations for future shows higher amount of curtailment mainly pertaining to very high volume of installation of wind power. However, the volume of wind power curtailed is still low as compared to the total amount of wind power generation. This being the reason, there is no seasonal pattern in the curtailment of wind power in future scenarios.

Simulations have shown that in future, hour ahead imbalance due to wind forecast error increases in Denmark mainly in DK1. However, the hour ahead imbalance for the whole synchronous area does not increase much. Therefore, intra-hour balancing of Danish control area is largely supported from neighbouring regions. Balancing cost which is highly driven by $CO_2$ prices in the simulation, increases substantially towards 2030. Balancing reserves in CE are largely provided by Natural Gas technologies whereas, in Nordic network, balancing reserves come from Hydro and Natural Gas. Balancing reserves in Denmark mainly come from Natural Gas. However, wind power also increases their role in balancing process in future, mainly in down regulation but also in up regulation especially if wind power is already curtailed in the day-ahead operation.

Real time imbalance seen by Nordic network increases multiple times in 2030 and 2050 scenario as compared to 2020 scenario. Additionally, the real time imbalance in Offshore grid scenario is much lower than that of Project based scenario. Nordic network is also expected to have much lower inertia available in future scenarios as compared to 2020 scenario.

The requirement for automatic frequency restoration reserves increases manifold in future scenarios as compared to 2020 scenario. Probabilistic dimensioning of frequency restoration reserves can be beneficial to mitigate the imbalances caused by wind power forecast error mainly in Nordic network. Even with proper dimensioning of frequency restoration reserves, frequency containment reserve for normal operation in Nordic network might be required to be increased in future 2030 and 2050 scenario with very high share of renewables in the power system.

**Contract no.:**

Grant no. 64018-0032 (EUDP, Danish energy Agency)

**Project no.:**

43277

**Sponsorship:** EUDP (previously ForskEL)

**ISBN**: 978-87-93549-67-8

**Pages: 76**

**Tables:** 17

**References:** 17

**Technical University of Denmark**
Department of Wind Energy,
Frederiksborgvej 399, Building 118,
4000 Roskilde Denmark

www.vindenergi.dtu.dk

kdas@dtu.dk

# Preface

The work presented in this report is deliverable D3.2 of the North Sea Offshore Network – Denmark (NSON-DK) project. The report is prepared in collaboration between DTU Wind Energy and DTU Management.

The NSON-DK project is funded by grant no. 64018-0032 under the EUDP program administrated by the Danish energy Agency (previously under ForskEL). It is carried out as a collaboration between DTU Wind Energy (lead), DTU Management and Ea Energy Analyses.

Authors would acknowledge their gratitude to Matti Koivisto for his support in this work.

# Contents

# Nomenclature

**Abbreviations**

$CHP$ Combined Heat and Power

$DA$ Day Ahead

$MILP$ Mixed Integer Linear Programming

$UC$ Unit Commitment

$VRE$ Variable Renewable Energy

**Sets**

$g \in \mathbb{GGG}$ Set of generation and pure storage units

$i \in \mathbb{I}$ Set of individual units

$y \in \mathbb{Y}$ Set of years

$s \in \mathbb{S}$ Set of seasons

$t \in \mathbb{T}$ Set of time steps

$a \in \mathbb{A}$ Set of areas

$c \in \mathbb{C}$ Set of countries

$r \in \mathbb{R}$ Set of regions

$ar \in \mathbb{AR}$ Areas in regions

$rc \in \mathbb{RC}$ Regions in countries

**Subsets**

$\mathbb{AFRD} \subset \mathbb{GGG}$ Set of technologies providing aFRR down regulation

$\mathbb{AFRU} \subset \mathbb{GGG}$ Set of technologies providing aFRR up regulation

$\mathbb{BP} \subset \mathbb{CHP}$ Set of CHP Back Pressure generation units

$\mathbb{CHP} \subset \mathbb{GD}$ Set of CHP units

$\mathbb{EL} \subset \mathbb{GGG}$ Set of technologies delivering electricity to consumers

$\mathbb{EXT} \subset \mathbb{CHP}$ Set of CHP Extraction generation units

$\mathbb{FCRD} \subset \mathbb{GGG}$ Set of technologies providing FCR down regulation

$\mathbb{FCRU} \subset \mathbb{GGG}$ Set of technologies providing FCR up regulation

$\mathbb{GD} \subset \mathbb{G}$ Set of dispatchable generation units

$\mathbb{GI} \subset \mathbb{G}$ Set of intermittent generation units

$\mathbb{HEAT} \subset \mathbb{GGG}$ Set of technologies delivering heat to consumers

$\mathbb{HO} \subset \mathbb{GD}$ Set of heat only generation units

$\mathbb{HYD} \subset \mathbb{GD}$ Set of hydro storage with hydro inflow generation units

$\mathbb{MFRD} \subset \mathbb{GGG}$ Set of technologies providing mFRR down regulation

$\mathbb{MFRU} \subset \mathbb{GGG}$ Set of technologies providing mFRR up regulation

$\mathbb{MRRD} \subset \mathbb{GGG}$ Set of technologies providing mRR down regulation

$\mathbb{MRRU} \subset \mathbb{GGG}$ Set of technologies providing mRR up regulation

$\mathbb{PO} \subset \mathbb{GD}$ Set of power only generation units

$\mathbb{PTOH} \subset \mathbb{HO}$ Set of power to heat generation units

$\mathbb{SLOW} \subset \mathbb{GGG}$ Set of technologies that do not participate in the balancing market

$\mathbb{G} \subset \mathbb{GGG}$ Set of generation units

$\mathbb{STO} \subset \mathbb{GGG}$ Set of pure storage units

**Parameters**

$\overline{HSL}_{a,s}$ Maximum seasonal hydro reservoir level [MWh]

| | |
|---|---|
| $\underline{HSL}_{a,s}$ | Minimum seasonal hydro reservoir level [MWh] |
| $AF_{g,a,y,s,t}$ | Availability factor of units [-] |
| $CB_g$ | Power-to-heat ratio [-] |
| $CV_g$ | Iso-fuel constant [-] |
| $D^{el}_{y,r,s,t}$ | Exogenous gross electricity consumption rate [MW] |
| $D^{h}_{a,y,s,t}$ | Exogenous gross heat consumption rate [MW] |
| $EC_{g,a,y}$ | Installed energy capacity for pure storage units [MWh] |
| $FC_{g,a,y}$ | Installed input fuel consumption capacity [MW] |
| $HI_{a,y,s}$ | Seasonal hydro inflow [MWh] |
| $HL_g$ | Hours to load pure storage units without losses[hours] |
| $HU_g$ | Hours to unload pure storage units without losses [hours] |
| $MDT_g$ | Minimum down time [hours] |
| $MMT_g$ | Minimum maintenance time [days] |
| $MO_g$ | Minimum operation point of a generation, storage loading, or storage unloading unit relative to unit size [-] |
| $MUT_g$ | Minimum on time [hours] |
| $SL_s$ | Season length [days] |
| $SO_{g,i}$ | Stochastic outage probability of single units [-] |
| $TCR_{r,r',y,s,t}$ | Transmission capacity rating [-] |
| $TL_{s,t}$ | Time step length [hours] |
| $US^{gen}_{g,a,y,s,t}$ | Unit size of input fuel capacity of a generation unit [MW] |
| $US^{sto}_{g,a,y,s,t}$ | Unit size of a storage unit [MWh] |
| $\eta^{h}_{g}$ | Thermal efficiency [-] |
| $\eta^{el}_{g}$ | Electric efficiency [-] |
| $\eta^{sto}_{g}$ | Storage cycle efficiency [-] |
| $C^{CO_2}_{g,a,y}$ | $CO_2 taxcost[€/MWh]$ |
| $C^{fom}_{g,a,y}$ | Fixed cost [€/MW for generation units, €/MWh for storage units] |
| $C^{fom}_{g}$ | Fixed cost [€/MW for generation units, €/MWh for storage units] |
| $C^{f}_{g,a,y}$ | Fuel cost [€/MWh] |
| $C^{on}_{g}$ | Online cost [€/MW] |
| $C^{oper}_{g,a,y}$ | Operational cost [€/MWh] |
| $C^{oper}_{g}$ | Operational cost [€/MWh] |
| $C^{sd}_{g}$ | Shut down cost [€/MW] |
| $C^{su}_{g}$ | Start up cost [€/MW] |
| $C^{trans}_{g,r,r',y}$ | Transmission cost [€/MWh] |
| $\overline{TMF}$ | Maximum start time requirement for mFRR [h] |
| $\overline{TMR}$ | Maximum start time requirement for mRR [h] |
| $\underline{\text{AFR}}$ | Minimum ramping requirement for aFRR [-] |
| $\underline{\text{FCR}}$ | Minimum ramping requirement for FCR [-] |
| $\underline{\text{MFR}}$ | Minimum ramping requirement for mFRR [-] |
| $\underline{\text{OAF}}$ | Minimum time unit needs to be "on" to deliver aFRR (hours) [h] |
| $\underline{\text{OFC}}$ | Minimum time unit needs to be "on" to deliver FCR (hours) [h] |
| $\text{AFR}^{dn}_{y,r}$ | aFRR required- down regulation in each hour [MW] |
| $\text{AFR}^{up}_{y,r}$ | aFRR required- up regulation in each hour [MW] |
| $\text{FCR}^{dn}_{y,r}$ | FCR required- down regulation in each hour [MW] |
| $\text{FCR}^{up}_{y,r}$ | FCR required- up regulation in each hour [MW] |
| $\text{MFR}^{dn}_{y,r}$ | mFRR required- down regulation in each hour [MW] |
| $\text{MFR}^{up}_{y,r}$ | mFRR required- up regulation in each hour [MW] |
| $\text{MRR}^{dn}_{y,r}$ | mRR required- down regulation in each hour [MW] |
| $\text{MRR}^{up}_{y,r}$ | mRR required- up regulation in each hour [MW] |
| **Positive decision variables** | |
| $d^{f}_{g,a,y,s,t}$ | Fuel consumption rate [MW] |

$n^{av,on}_{g,a,y,s,t}$ Number of units available for generation online [-]

$n^{av,sd}_{g,a,y,s,t}$ Number of units available for generation shutting down [-]

$n^{av,su}_{g,a,y,s,t}$ Number of units available for generation starting up [-]

$n^{nav,pm,sd}_{g,a,y,s,t}$ Number of units not available for generation stopping maintenance [-]

$n^{nav,pm,su}_{g,a,y,s,t}$ Number of units not available for generation starting maintenance [-]

$n^{nav,pm}_{g,a,y,s,t}$ Number of units not available for generation on maintenance [-]

$p^{el}_{g,a,y,s,t}$ Net delivered power [MW]

$p^{h}_{g,a,y,s,t}$ Net delivered heat [MW]

$so_{g,a,y,s,t,i}$ Stochastic outage of single units [-]

$stol_{g,a,y,s,t}$ Storage loading rate [MW]

$ston^{av,on}_{g,a,y,s,t}$ Number of available units for loading pure storage online [-]

$ston^{av,sd}_{g,a,y,s,t}$ Number of available units for loading pure storage shutting down [-]

$ston^{av,su}_{g,a,y,s,t}$ Number of available units for loading pure storage starting up [-]

$afrr^{dn}_{g,a,y,s,t}$ aFRR-down regulation power reserved [MW]

$afrr^{up}_{g,a,y,s,t}$ aFRR-up regulation power reserved [MW]

$c^{CO_2}_{g,a,y}$ $CO_2$ tax annual cost [€/MWh]

$c^{fom}_{g,a,y}$ Fixed annual cost [€/MW for generation units, €/MWh for storage units]

$c^{trans}_{g,a,y}$ Transmission annual cost [€/MWh]

$c^{uc}_{g,a,y}$ Unit commitment related annual cost [€/MW]

$c^{vom}_{g,a,y}$ Variable Operational annual cost [€/MWh]

$fcr^{dn}_{g,a,y,s,t}$ FCR-down regulation power reserved [MW]

$fcr^{up}_{g,a,y,s,t}$ FCR-up regulation power reserved [MW]

$hsl_{a,y,s}$ Hydro reservoir energy level [MWh]

$mfrr^{dn}_{g,a,y,s,t}$ mFRR-down regulation power reserved [MW]

$mfrr^{up}_{g,a,y,s,t}$ mFRR-up regulation power reserved [MW]

$mrr^{dn}_{g,a,y,s,t}$ mRR-down regulation power reserved [MW]

$mrr^{up}_{g,a,y,s,t}$ mRR-up regulation power reserved [MW]

$soc_{g,a,y,s,t}$ State of charge of pure storage [MWh]

# Chapter 1

# Introduction

The share of variable renewable energy (VRE) sources, like wind and solar is expected to increase and become major energy resources towards the fossil fuel free energy system. Particularly, in the North Sea a massive offshore wind penetration is expected. The increase of the variable renewable energy sources in the grid brings new conditions to the energy system due to the inherent variability and forecast uncertainty. Power imbalances due to uncertainty of the VRE poses major challenges for the reliability and security of power system.

In principal, the penetration of VRE is challenging the operation of traditional electricity systems due to several facts. The marginal cost of VRE is normally lower than the conventional power plant's one, leading to lower bids coming from the VRE generators which means that generally VRE will be dispatched before most thermal power plants. Thus, thermal power plants with high fixed costs could become unprofitable and shut down, limiting systems adequacy. Additionally, with the increase of VRE share in the energy mix, balancing requirements close to real time are expected to expand due the forecast errors challenging the security of supply. One of the major challenges involve balancing of the power system with large share of VRE. To evaluate the impact of variability of VRE sources and imbalances caused by VRE forecast uncertainties, a complete chain of operations need to be modelled comprising of day-ahead market operation, intra-hour balancing operation and automatic frequency control. This report encompasses all these operations through modelling for all the North Sea countries for multiple scenarios of future energy systems.

The electricity system in Europe consists of three major types of markets which differentiate themselves on the time scale of the trading being made prior to real time delivery. First, is the Day Ahead (DA) electricity market which is the one where the majority of the energy is traded and is run daily. In this market, the buyers estimate the amount of energy they will demand for each hour of the next day and place their bid based on how much they are willing to pay for it. Similarly, sellers estimate the amount and price of the energy that they will be able to offer for every hour of the following day. Producers and consumers participate on the market and then the hourly prices are cleared and the generation schedule of the next day is created.

As expected, the forecasts done from both the buyers and sellers during the DA electricity market are likely to be changed closer to the real time delivery and that is mainly caused due to Day Ahead VRE forecast error. For that reason, the Intra-Hour (IH) market

is run an hour ahead from the real time. The scope of this market is to efficiently balance the imbalance caused due to the DA forecast error using the updated hour-ahead forecasts.

Even the hour-ahead VRE generation forecasts diverge from the real time VRE generation. The imbalances that will inevitably occur at the delivery time are handled by the automatic reserves. The deployment of the automatic reserves is simulated from the Area Control Model whose main purpose is to limit the frequency change following a disturbance.

This report analyses a) the value of future wind power development in North sea countries (project based and offshore grid scenarios) on balancing of forecast errors, b) the impact of forecast errors on manual and automatic reserves and c) the quality of the electrical frequency for prognosed energy scenarios of 2020, 2030 and 2050. This is accomplished by creating a balancing tool chain simulating the three stages of power system operation described above. The report is part of the WP3 of the NSON-DK project [1] and the scenarios used are the ones developed in WP2 [2]. The NSON-DK project studies the impact on the system of VRE expansion in the short, medium, and long term, focusing on the Danish power system.

# Chapter 2

# Balancing Tool Chain

The scope of this report is to study the impact of the VRE penetration in the power system. Hence, all stages of power system operation (Day Ahead, Intra-Hour, Real Time frequency control) required to be modeled. A Balancing tool chain [3] is developed whose structure is shown in Fig. 2.1.

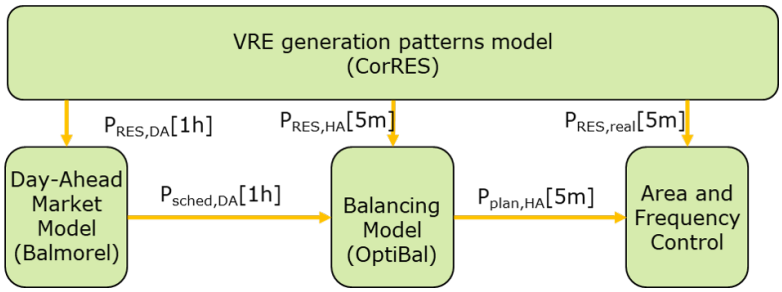


Figure (2.1) The tool-chain structure.

VRE generation is simulated via DTU Wind Energy software CorRES [4] with time series that provide the available energy during each time step. CorRES is is used to generate DA forecast error simulation, HA forecast error simulation and real time available power for wind power.

The simulation of the DA market operation is performed with the Balmorel open source energy system model [5] and the optimizations are carried out with a rolling seasonal horizon approach of one day. Balmorel model uses as input the VRE DA forecasts calculated from CorRES with hourly resolution. Based on these forecasts, the DA market is run and an hourly generation schedule is created.

Optibal receives as input both the hour ahead wind forecasts in 5 minutes time steps from CorRES and the hourly generation plan from Balmorel. The DA wind dispatches are compared with new forecasts and the instantaneous system's imbalance is calculated. Then OptiBal's optimization algorithm calculates the required generation adjustments in order for the hour ahead imbalance to be minimized. Both Balmorel and OptiBal use the Unit Commitment (UC) methodology in order to obtain a realistic behaviour of generations respecting the ramping and other UC constraints.

Lastly, a dynamic model is built in order to analyse deployment of the automatic reserves. The Area and Frequency Control model takes as input the Real Time VRE generation (in

5 minutes time steps) as calculated from CorRES and the new generation plan created from OptiBal (in 5 minutes time steps). With these inputs, the real time imbalance can be determined and interpolated in 1 second time steps in order for the dynamic model to simulate the automatic reserves deployment and the real time frequency deviations.

These tools are explained in details in next chapters.

# Chapter 3

# NSON-DK Scenarios

This chapter provides a brief overview of the scenarios used in this report. A more detailed description of these scenarios can be found in [2].

## 3.1 Countries in focus

As already mentioned, the objective of NSON-DK project is to study how the offshore wind energy development in the North Sea affects the Danish power system. Despite that Denmark is the main focus, modelling its neighboring countries is also important since electricity systems are heavily interconnected. The countries for which the electricity generation and transmission development was optimized in WP2 of the NSON-DK project are : Denmark, Norway, Great Britain, Netherlands, Belgium and Germany. On the other hand, the development of other surrounding countries, such as Poland, Sweden, Finland, Estonia, Latvia and Lithuania, was not optimized but assumed. These are all the countries included in the DA and IH market optimization performed for this report. The participating countries are split in bidding regions and thus Denmark is divided to DK1 (West) and DK2 (East) respectively.

The Frequency Control is performed in the synchronous area level. The geographical area covered by ENTSO-E's (European Network of Transmission System Operators) member TSOs is separated into five synchronous areas and two isolated systems (Cyprus and Iceland). Denmark's regions (DK1 and DK2) belong to different synchronous areas, Continental Europe (CE) and Nordic respectively. Since, the scope of this report is to examine the impact of the offshore wind energy development on the Danish power system, only countries mentioned before are considered at the Area and Frequency Control model. Thus, in this report CE consists of Belgium, Germany, Netherlands, Poland and Denmark's region DK1. Similarly, the Nordic synchronous area includes Norway, Sweden, Finland and DK2.

## 3.2 Project-based and offshore grid scenarios

The scenarios used for these studies are based on investment optimization for generation and transmission capacity for North Sea countries. A project-based scenario and an offshore grid scenario were developed in the NSON-DK project. As shown in Fig.3.1, these scenarios are differentiated by the allowed offshore grid structure. In the investment optimization of

the project-based scenario only radial offshore connections are permitted. On the contrary, the offshore grid scenario includes both radial and meshed offshore connections via hubs.

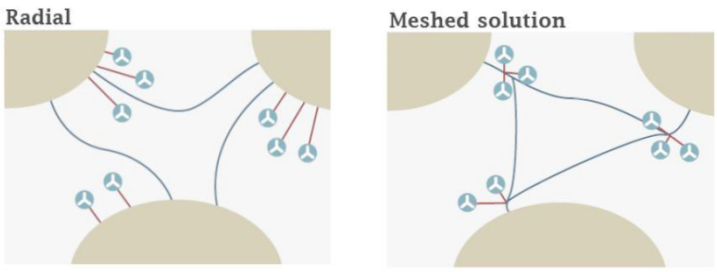


Figure (3.1) Schematic of project-based ("radial") and offshore grid ("meshed") connection structures [6].

The resulting transmission development in the North Sea region towards 2050 for the project-based scenario is depicted in Fig.3.2. As shown, the level of interconnection between the studied countries is high and especially to Norway. Connections with Norway proved to be crucial since its hydro power can be used not only to cover its domestic demand, but also to provide flexibility to its neighbors.

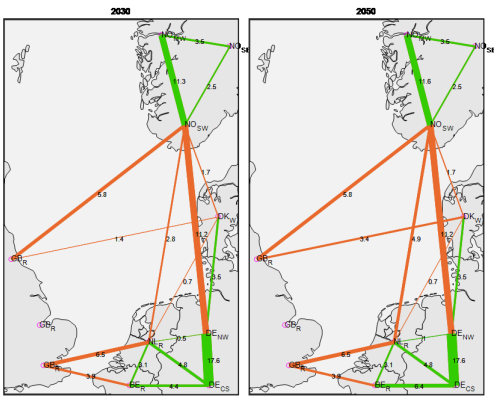


Figure (3.2) Project-based scenario: transmission lines in 2030 and 2050 (GW) between regions visible in the map. On-land lines in green and country-to-country offshore lines in orange. [2]

Similarly, the resulting transmission development for the offshore grid scenario is illustrated in Fig. 3.3. Again, the investment optimization concluded in highly interconnected countries but in this case except the country-to-country (C2C) direct connections, C2C connections via hubs were also chosen. Hub connected lines have the advantage that their transmission capacity could be used for both wind offshore dispatch and C2C trade.

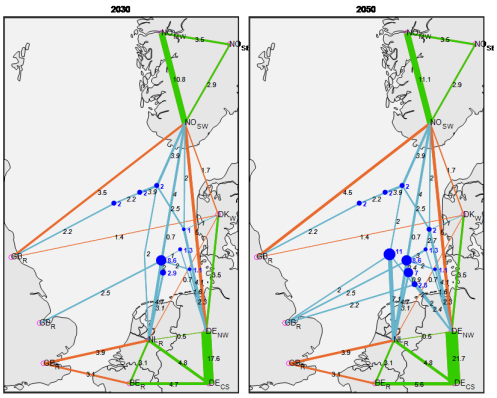


Figure (3.3) Offshore grid scenario: transmission lines and hubs in 2030 and 2050 (GW) between regions visible in the map. On-land lines in green, C2C offshore lines in orange, lines related to the meshed grid in light blue and hubs in dark blue. [2]

The development of aggregated electricity generation capacity per fuel type towards 2050 in the countries in focus for the project-based and offshore grid scenarios is presented in Fig.3.4. The starting point for modelling the generation capacity are the expected installed capacities by 2020. The generation capacity develops for the years 2030 and 2050 through the investment optimization of the model [2]. The offshore grid shows a 10.3 GW increase of wind offshore capacity by 2050. In the other hand, the project-based scenario presents higher capacities for onshore wind (7.8 GW), solar PV (6.5 GW) and fossil thermal power(8.2 GW). The fact that the offshore grid scenario end up with reduced fossil thermal power capacity indicates that this type of connection structures are more efficient in providing flexibility to the system.

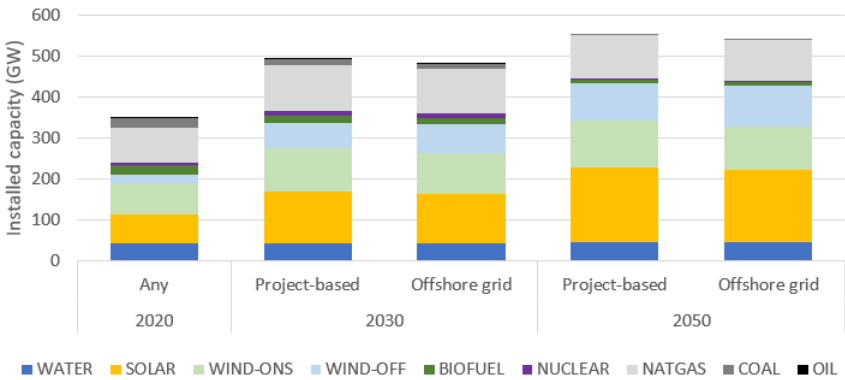


Figure (3.4) Installed electricity capacity development per fuel and scenario in the countries in focus (GW). [2]

The development of the installed electricity capacity per fuel type towards 2050 in control areas DK1 and DK2 are illustrated in figures 3.5 and 3.6 respectively. As shown, DK1 holds higher installed capacities of wind technologies compared to DK2 both in absolute and in relative terms. Thus, DK1 is expected to experience larger imbalances in all scenarios. The highest share of installed wind capacity in respect to the aggregated installed electricity generation capacity for DK1 and DK2 is presented in offshore grid scenario 2030 with

71.4% and in project based 2050 with 32.9% respectively.

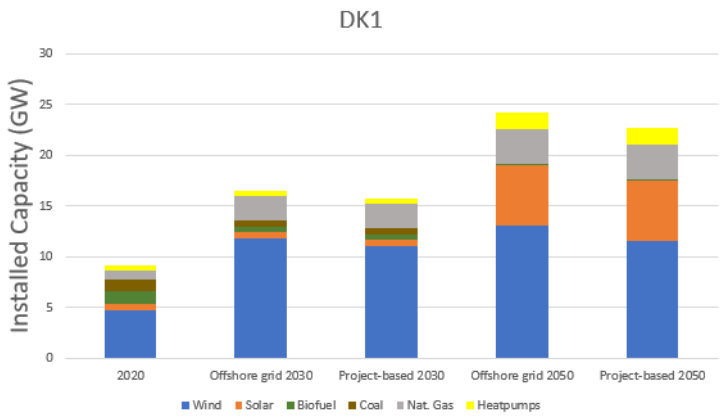


Figure (3.5) Installed electricity capacity development per fuel and scenario DK1 (GW). [2]

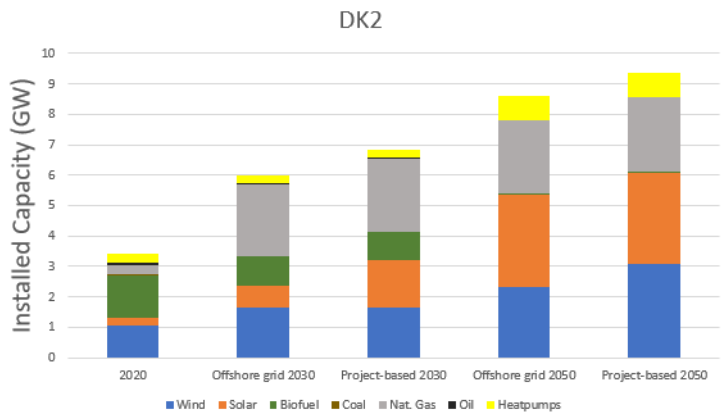


Figure (3.6) Installed electricity capacity development per fuel and scenario in DK2 (GW). [2]

# Chapter 4

# CorRES

CorRES (Correlations in Renewable Energy Sources) simulation tool is used to calculate the VRE generation time series presented in this report. CorRES is capable of simulating both wind and solar generation by using a combination of meteorological time series and stochastic simulations to create consistent VRE generation and forecast error time series [7]. For this report, the wind generation forecasts of the next day (DA market) are generated with temporal scale of 1 hour. The forecasts of the next hour (IH market) and the realization of the wind are generated with temporal resolution of 5 minutes (only the wind generation is considered uncertain).

## 4.1 Comparison among scenarios

The aggregated Real Time available wind generation in TWh for the whole year in each scenario is given in table 4.1 while installed capacity for all the scenarios are given in [2]. The available wind power increases in both scenarios towards 2050 following the trend of the installed wind capacity.

| Real Time available Wind (TWh) | | | | | |
|---|---|---|---|---|---|
| | | Offshore Grid | | Project-based | |
| **Control & Synchronous Areas** | **2020** | **2030** | **2050** | **2030** | **2050** |
| **BELGIUM** | 12 | 37 | 37 | 37 | 37 |
| **ESTONIA** | 2 | 2 | 1 | 2 | 1 |
| **FINLAND** | 6 | 6 | 6 | 6 | 6 |
| **FRANCE** | 124 | 124 | 208 | 124 | 208 |
| **GERMANY** | 155 | 239 | 344 | 179 | 229 |
| **GREAT BRITAIN** | 76 | 175 | 200 | 186 | 203 |
| **NETHERLANDS** | 18 | 18 | 20 | 53 | 91 |
| **LATVIA** | 7 | 7 | 6 | 7 | 6 |
| **LITHUANIA** | 4 | 4 | 15 | 4 | 15 |
| **NORWAY** | 11 | 54 | 76 | 52 | 85 |
| **POLAND** | 67 | 67 | 67 | 67 | 67 |
| **SWEDEN** | 29 | 29 | 59 | 29 | 59 |
| **DK1** | 16 | 46 | 52 | 43 | 45 |
| **DK2** | 4 | 5 | 9 | 5 | 12 |
| **CE** | 392 | 531 | 729 | 503 | 678 |
| **NORDIC** | 49 | 94 | 150 | 92 | 162 |

Table (4.1) The aggregated Real Time available wind generation for each control and synchronous area in each scenario scenario in TWh.

## 4.2 Analysis of forecast errors

The Day Ahead forecast error is defined in this report as the difference between the Day Ahead forecasts from the Real time available wind. The probability density function plots of the DA forecast error in DK1 and DK2 for each scenario and year is depicted in figures 4.1 and 4.2 respectively. It can be observed that DA forecast error increases towards 2050 as the installed capacity of wind technologies expands too. As was expected, DK1 presents higher forecast error compared to DK2 in all of the scenarios and years since DK1 has more installed capacity of wind as compared to DK2. Substantial increase of DA forecast error implies the value of studies (as done in this report) to quantify the requirements of different types of reserves for mitigating these imbalances in future scenarios.

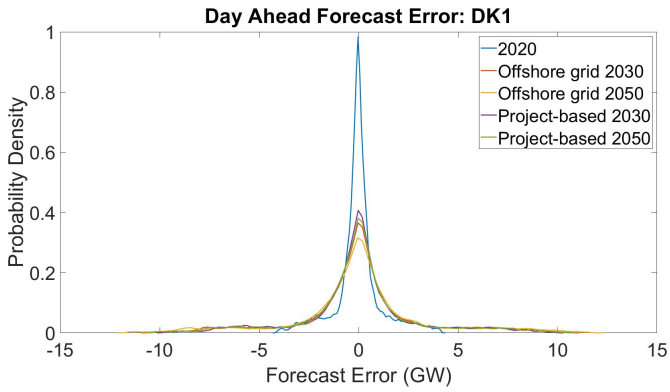


Figure (4.1) Probability density of Day Ahead forecast error (Real Time - Day Ahead forecast) of DK1 control area for each scenario and year.

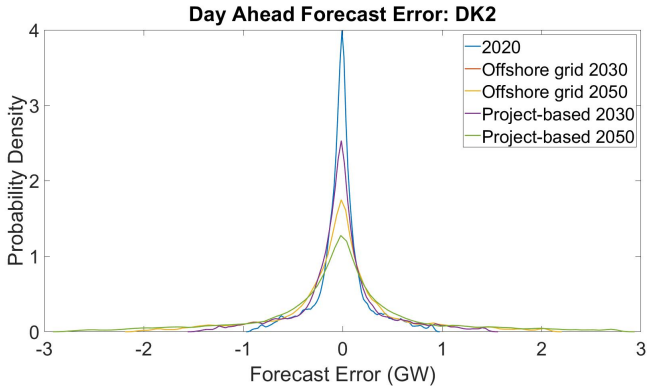


Figure (4.2) Probability density of Day Ahead forecast error (Real Time - Day Ahead forecast) of DK2 control area for each scenario and year.

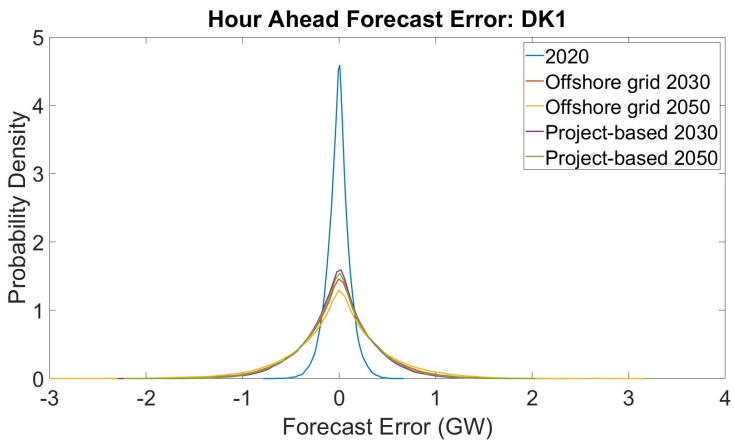


Figure (4.3) Probability density of Hour Ahead forecast error (Real Time - Hour Ahead forecast) of Denmark DK1 control area for each scenario and year.

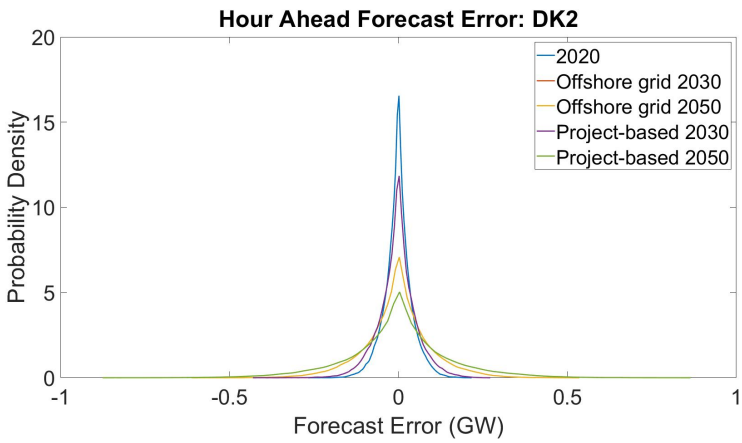


Figure (4.4) Probability density of Hour Ahead forecast error (Real Time - Hour Ahead forecast) of Denmark DK2 control area for each scenario and year.

The probability density function plots of the Hour Ahead forecast error in DK1 and DK2 for each scenario and year is depicted in figures 4.1 and 4.2 respectively. Since, the forecasts

improve closer to the real time, forecast error reduces in Hour Ahead as compared to Day Ahead forecast. Therefore, it shows the value of intra-hour balancing which in turn would reduce the requirements for real-time reserves. It should also be noted that Hour Ahead forecast error for 2050 scenarios for Denmark is much more than that of 2020 but almost equivalent to 2030. The reason for this is not much wind power is installed in Denmark between 2030 and 2050.

These plots show the motivation for quantification of the reserve requirements for different future scenarios as discussed in details in following chapters.

# Chapter 5

# Day Ahead Market Model-Balmorel

## 5.1 Methodology

The model presented in this report includes both elastic and inelastic demand. There are two kinds of generators participating in the Day Ahead market, the dispatchable generators and the non-dispatchable. Thermal power plants (power-only or cogeneration), boilers, heat pumps and electric boilers are considered dispatchable. In contrary, wind, solar PV, hydro run-of-river,power interconnectors, heat and electricity storage units consist the non-dispatchable generators. The methodology and the mathematical equations are described in details in Appendix A.

The Day-Ahead market optimisation is performed on a daily basis to replicate the behaviour of the spot market of electricity. The results are linked from day to day, which means that what happened in the previous days may limits what can happen in a particular day. This limitation is highly dependent on the flexibility of the different units.

Major results for Day-Ahead market operation has been published in [8]. Additional results relevant for balancing process are additionally reported in this report in the following sections.

## 5.2 Comparison among scenarios

In this section, the results of the Day Ahead market optimization are presented and compared among the different scenarios and years of simulation.

### 5.2.1 Wind Power Curtailment

During the Day Ahead market, the optimization algorithm is allowed to curtail wind generation. Since wind technologies present low operational cost the model tries through the optimization algorithm to cover as much as possible of the electricity demand with wind energy. Even if the demand for electricity is lower than the available wind energy in a particular region, the model will export the surplus to the neighboring regions if possible in the specific time step. Wind generation will be curtailed only in cases that a part of the

wind available generation is not possible to be used domestically or to be exported.

For better understanding of the conditions causing the wind to be curtailed, we need to focus on one specific time step of the optimization procedure. For example, based on the results of the simulation, at the $4^{th}$ of January 2020 between 22:00 and 23:00, $13MWh$ of available wind energy are curtailed in DK1 control area. At the time step 22:00, the exogenous and the endogenous (electricity to heat) electricity demand is $2460MW$ and $184MW$ respectively thus $2644MW$ in total. The Day Ahead forecast predict $4450MW$ of available wind power for the same time step. Since the wind generation is expected to be higher than the demand the optimization algorithm decides to export as much as possible to the neighboring countries. Thus, the interconnection lines from DK1 to DK2, HOLLAND, NORWAY and SWEDEN are operating on their maximum exporting in total $3553MW$. The algorithm didn't export energy to GERMANY because of low demand requirement in GERMANY at the same time. Thus, for the aforementioned time step the imports of DK1 are equal with $1268MW$. Due to unit commitment constrains and for automatic reserve adequacy purposes (the automatic reserves have to be scheduled before the Day Ahead market in order to be deployed at the Real Time) a part of the demand should be covered from technologies other than wind. Thus, on that specific time step the aggregated generation from non wind technologies is $492MW$. So, in order the generation-demand balance to be achieved $4437MW$ $(2644MW + 3553MW - 1268MW - 492MW)$ of wind power are dispatched leading to $13MW$ of wind power curtailed.

The aggregated monthly wind energy curtailed in all countries of simulation for each scenario and year is depicted in figure 5.1. It can be observed that by 2020 the most of the curtailment occurs in autumn and winter (October to March). There is however a small peak in June, owing to low demand situations. Moreover, towards 2050 the curtailment increases but no clear seasonal patterns can be observed. It seems that, by 2050, the penetration of VRE is so high, that low demand situations are quite likely to lead to curtailment. Although, the amount of curtailment is still high for January, June and December. Offshore grid scenario has a little bit higher curtailment as compared to project based scenario in 2050. The reason for this is slightly higher volume of wind power installation for offshore grid scenario as compared to project based scenario.

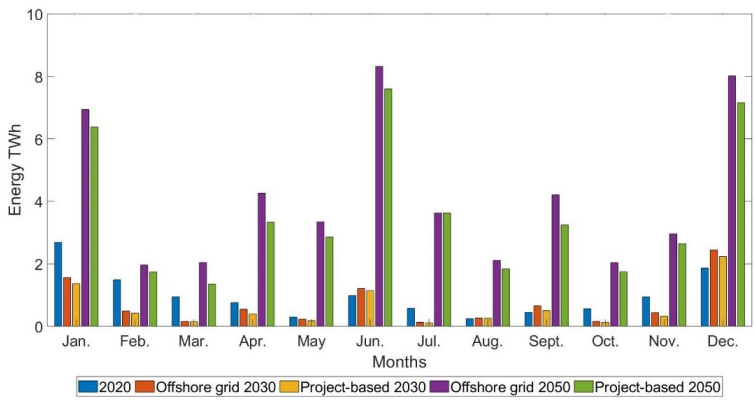


Figure (5.1) The Day Ahead aggregated monthly wind generation curtailment of all simulated countries for each scenario and year

The box and whisker diagram of the monthly wind power curtailed in DK1 and DK2 for each scenario is depicted in figures 5.2 and 5.3 respectively. As shown, there is no seasonal pattern in wind power curtailment in 2030 and 2050.

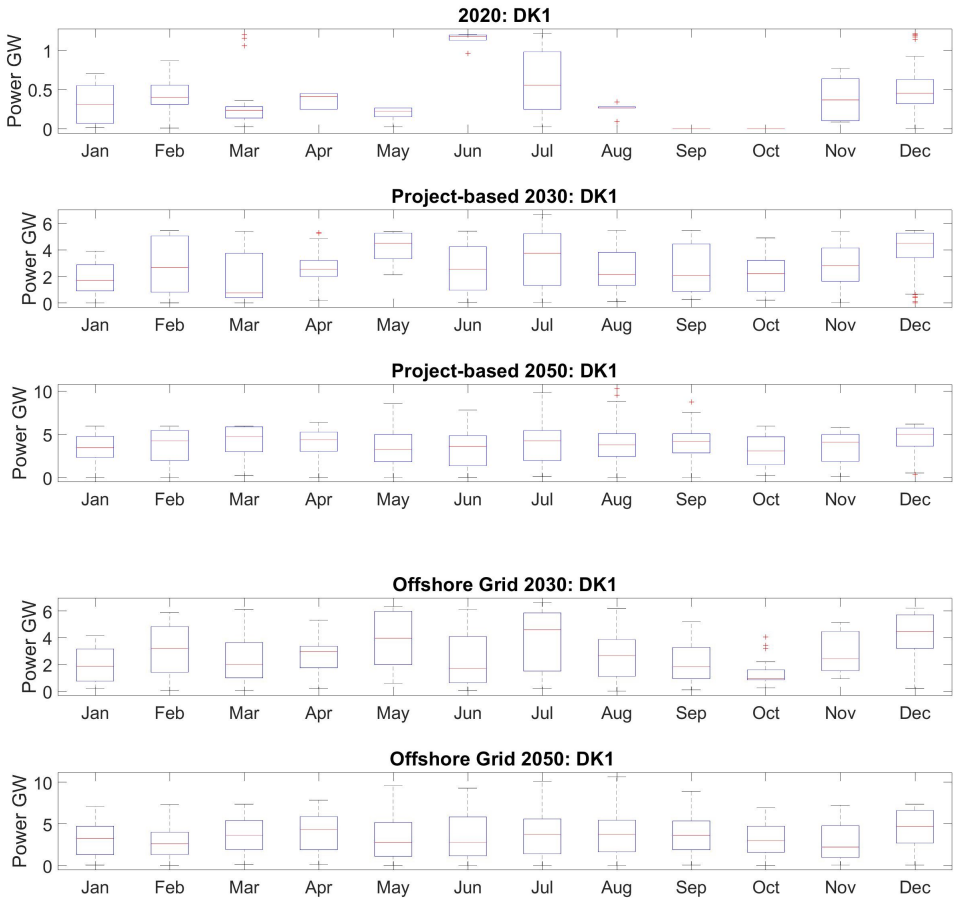


Figure (5.2) Box and whisker diagram of the monthly wind power (GW) curtailed in DK1 for each scenario and year.

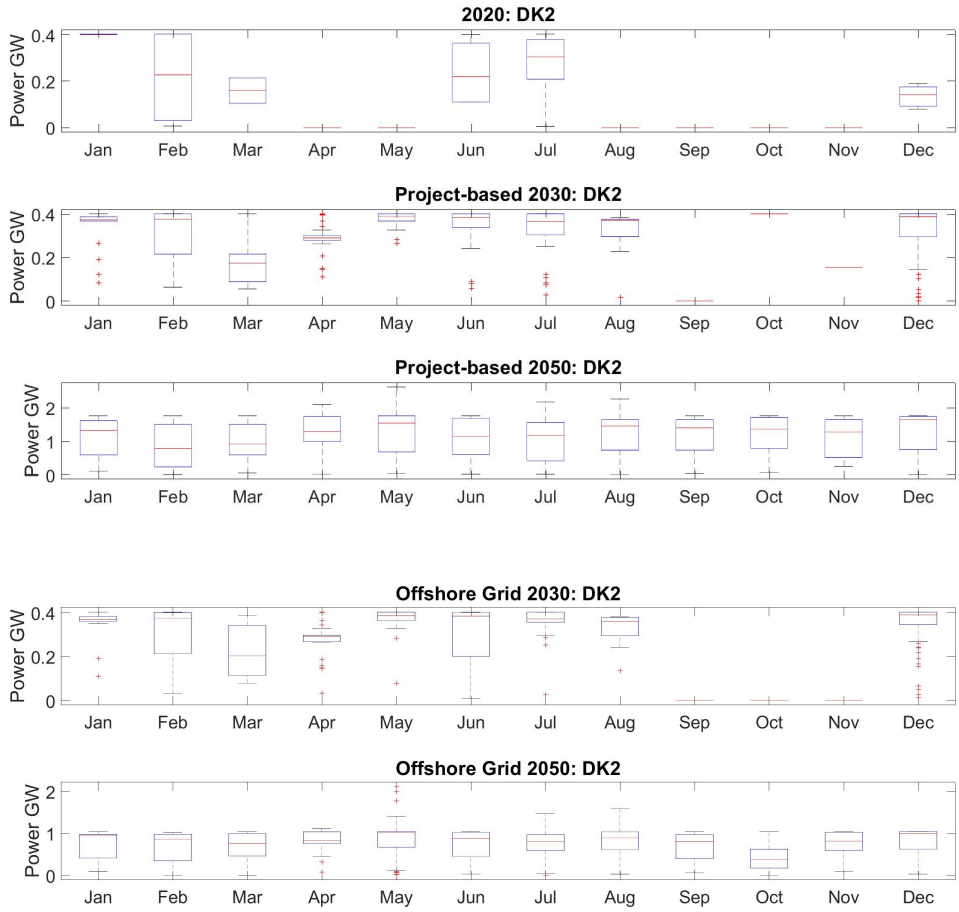


Figure (5.3) Box and whisker diagram of the monthly wind power (GW) curtailed in DK2 for each scenario and year.

Total amount of wind energy curtailed in each control area, scenario and year is presented in the table 5.1. As expected, since the wind generation expands towards 2050, the curtailed wind energy is increasing as well. The project-based scenario seems to perform better since the wind energy curtailed when aggregated in synchronous area level is lower compared with the offshore grid scenario.

**Day Ahead Curtailment (GWh)**

| | | Offshore Grid | | Project-based | |
|---|---|---|---|---|---|
| **Control & Synchronous Areas** | **2020** | **2030** | **2050** | **2030** | **2050** |
| **BELGIUM** | 0 | 752 | 3659 | 1020 | 4749 |
| **GERMANY** | 9605 | 6534 | 43941 | 3808 | 18750 |
| **NETHERLANDS** | 3 | 93 | 663 | 1278 | 14513 |
| **NORWAY** | 2 | 2033 | 9049 | 426 | 5118 |
| **SWEDEN** | 6 | 7 | 106 | 8 | 124 |
| **DK1** | 106 | 1691 | 6344 | 1866 | 6147 |
| **DK2** | 14 | 65 | 565 | 79 | 1060 |

Table (5.1) Day-ahead wind power curtailment for North Sea countries for future scenrios

### 5.2.2 Instantaneous Share of Wind Power

This section reports the results related to the instantaneous share of wind power generation in respect to the electricity demand. The cumulative distribution function of the fraction of Wind Power/Elctrecity Demand for each scenario and year for DK1 and DK2 are illustrated in figures 5.4 and 5.5 respectively. Regarding the control area DK1, the cumulative probability of 100% instantaneous electrical power provided from wind in 2020 is 65% and increases towards 2050 for both scenarios. In the other hand, in DK2, the instantaneous share of wind power never reaches 100% in 2020 but increases towards 2050 for both scenarios as well. This shows that Danish power systems are major exporter of energy, but also it has a relevance for balancing mechanism. With no or very low amount of conventional generators operating in the system, balancing responsibilities has to fall on wind power plants and fast startup generators.

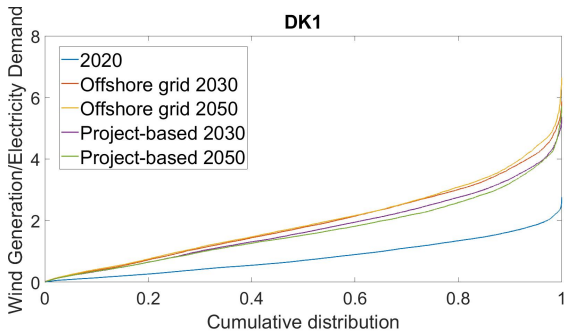


Figure (5.4) Cumulative distribution of the instantaneous share of wind power generation in respect to demand for each scenario and year in DK1.

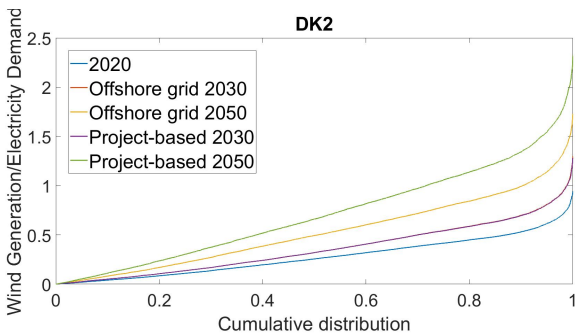


Figure (5.5) Cumulative distribution of the instantaneous share of wind power generation in respect to demand for each scenario and year in DK2.

Next, the box and whisker diagram of the instantaneous share of the wind power in respect to the demand for electric power, desegregated monthly, is presented for DK1 and DK2 in figures 5.6 and 5.7 respectively. Based on these results, no seasonal patterns can be observed in the instantaneous share of wind power. The last conclusion can be explained from the fact that it is common during the months with high wind penetration, the demand for electricity to be also higher.

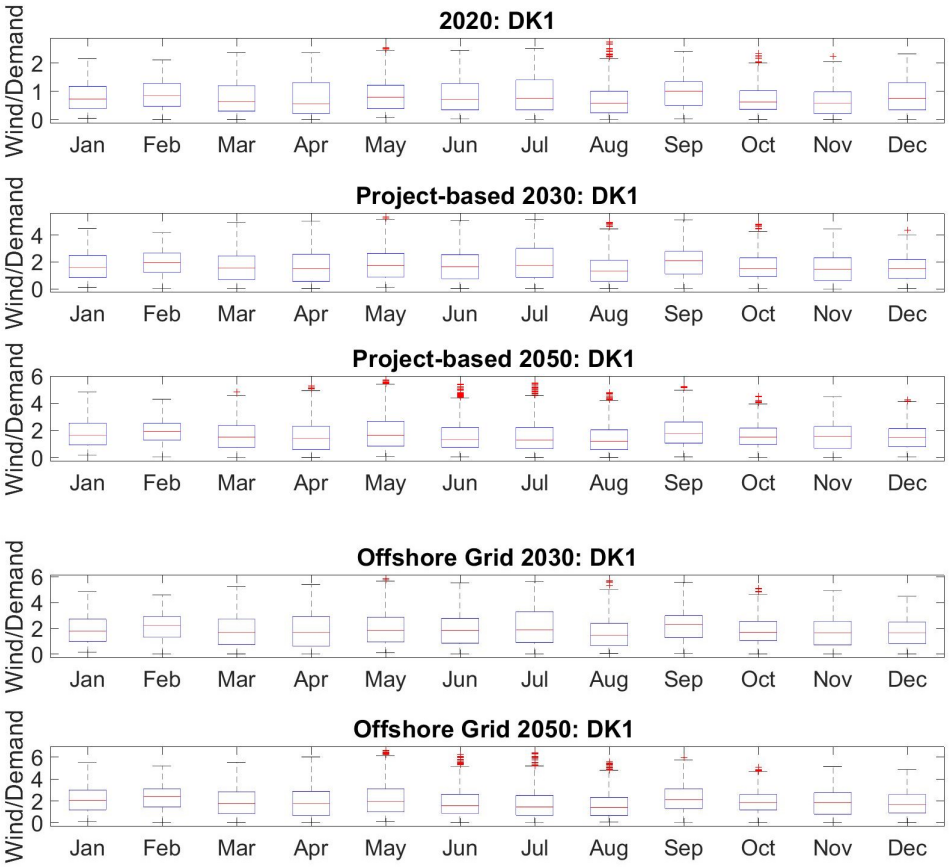


Figure (5.6) Box and whisker diagram of the monthly instantaneous share of wind power generation in respect to demand for DK1.


Figure (5.7) Box and whisker diagram of the monthly instantaneous share of wind power generation in respect to demand for DK2.

### 5.2.3 Electricity Prices

The seasonal variation of the electricity prices coming from the Day-Ahead market simulations is studied in this section. The box and whisker diagram of the electricity prices in each scenario and year, for the regions DK1 and DK2 are shown in figures 5.8 and 5.9 respectively. As illustrated, the electricity prices of DK1 and DK2 are almost identical due to the high level of interconnection between the two regions. As observed, during spring and summer months (April to September) the prices present lower mean values than the autumn and winter months (October to March). Electric energy is cheaper in spring and summer months because the demand for electricity is lower in these months compared to the colder months of winter and autumn. Additionally, based on these two figures, it is obvious that the mean values of the electricity prices increase from 2020 to 2030 and decrease from 2030 to 2050 for both scenarios. This development demonstrates the link between the electricity prices, the $CO_2$ price and the penetration of wind energy in the system. In 2030, electric energy coming from fossil fuels is still a considerable part of the energy mix and since the $CO_2$ price is increasing, electricity prices expand too. In contrary, in 2050 a larger share of the demand is covered from VRE technologies pushing the prices to decrease. Detailed analysis of electricity prices can be found in [8].

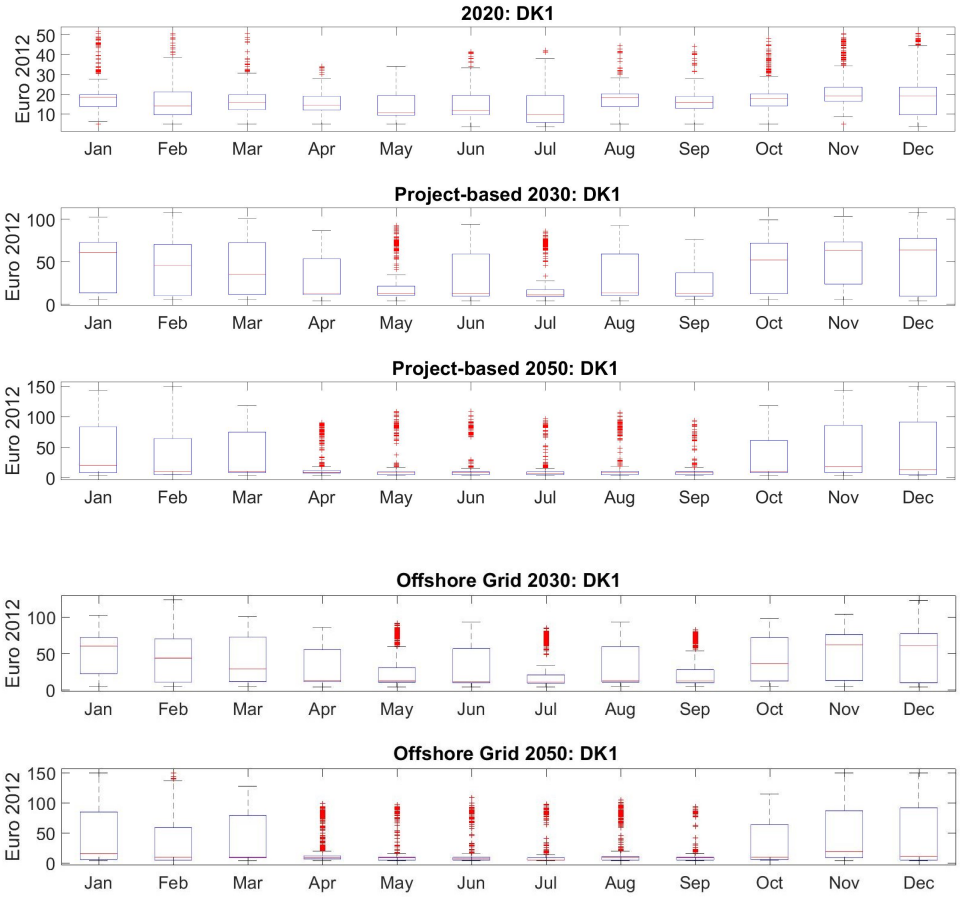


Figure (5.8) Box and whisker diagram of the monthly electricity price (Euro2012/MWh) in DK1 for each scenario and year.

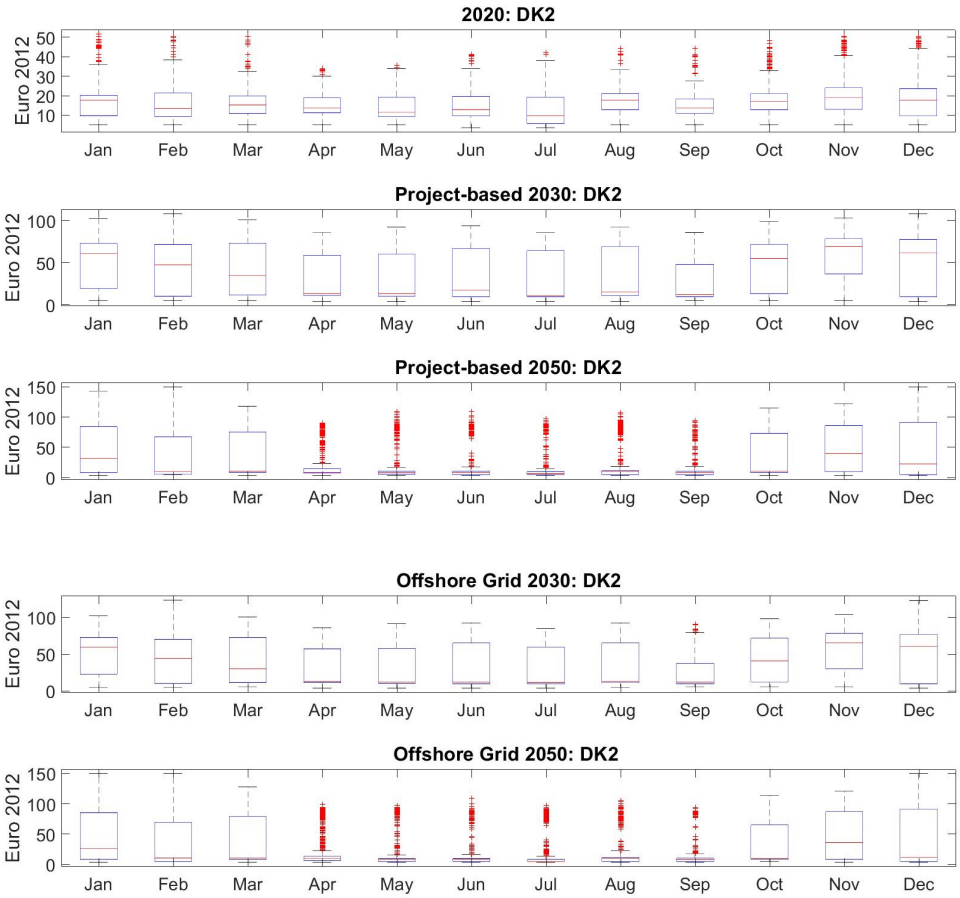


Figure (5.9) Box and whisker diagram of the monthly electricity price (Euro2012/MWh) in DK2 for each scenario and year.

### 5.2.4 Shortage of generation

As described before, the development of the installed electricity generation capacity of each region was modelled in WP2 of NSON-DK project based on investment optimization methods [2] based on 8 representative weeks. Despite that, during the optimization of the Day Ahead market there are time steps where the electricity demand could not be supplied due to inadequacy of generation sources or unavailability of transmission line capability. The number of hours that DK1 and DK2 experience shortage of generation are presented for each scenario and year in table 5.2.

**Hours with shortage of generation**

| | | Offshore grid | | Project-based | |
|---|---|---|---|---|---|
| **Control Area** | **2020** | **2030** | **2050** | **2030** | **2050** |
| **DK1** | 432 | 4658 | 28 | 4545 | 13 |
| **DK2** | 733 | 3 | 23 | 0 | 12 |

Table (5.2) Number of hours with shortage of generation in each control area, scenario and year

Next, the volume of the energy missing in DK1 and DK2 for each scenario and year is shown in table 5.3.

**Volume of shortage of generation (GWh)**

| | | Offshore grid | | Project-based | |
|---|---|---|---|---|---|
| **Control Area** | **2020** | **2030** | **2050** | **2030** | **2050** |
| **DK1** | 13 | 313 | 5 | 302 | 3 |
| **DK2** | 7 | 0 | 3 | 0 | 2 |

Table (5.3) Volume of missing electrical energy in each control area, scenario and year

It can be observed from the above tables that the volume of missing energy and number of hours are negligible in DK2. In DK1, there are hours when volume of energy is missing, mainly in 2030 scenarios. The reason for this is mainly not considering sector coupling in the investment optimization as well as due to the fact that investment optimization is performed based on 8 representative weeks.

# Chapter 6

# Intra Hour Balancing Model-OptiBal

Methodology and mathematical model of Intra-hour market and balancing is detailed in Appendix B. In this chapter, different scenarios are compared in terms of the input imbalance, the Intra-Hour (IH) clearing prices, the reserve activated and the number of hours with inadequate balancing reserves. The results are mainly shown for Denmark based on the scope of the project.

## 6.1 Methodology

The OptiBal model receives as input the hour ahead wind forecast simulations in temporal resolution of 5 minutes from CorRES and the hourly generation schedule from Balmorel. The main purpose of this model is to calculate the required adjustments from non VRE generators in order to counteract the imbalance occurred due to the mismatch of the DA wind dispatches and the new wind generation forecasts.

The methodology [9] used to simulate the Intra Hour market can be split in two groups: Fixing Balancing Variables add-on and the Balancing Market optimization. The Intra Hour balancing market optimisation is performed on a hourly basis. The results are linked from hour to hour meaning that the results of the previous hour may limit the results in the next hour. This limitation is highly dependent on the flexibility of the different units. The flexibility of the units, endogenously from the model, determines whether a unit is able to participate in the balancing market or not.

It is important to note that OptiBal is modelled based on Danish practices for all the other countries as well. This is not true in practice today, however, this is valuable and important in order to model the balancing reserves required for Denmark as well as the support from neighboring regions during balancing operation.

## 6.2 Comparison among scenarios

### 6.2.1 Analysis of input Imbalance

The evolution of the input imbalances towards 2050 for both project based and offshore grid scenarios in Continental Europe and Nordic synchronous areas are shown in figure 6.1 and 6.2 respectively. As shown, the volume of the imbalance follows the trend of the installed wind generation capacity development meaning that it is increasing towards 2050. The $5^{th}$ and the $95^{th}$ percentile values of the input imbalances are calculated in order to estimate the required balancing reserves. The physical significance of the $5^{th}$ percentile of the imbalance is that equals with the reserves required to counteract 95% of the negative imbalances occurred. Similarly, the $95^{th}$ percentile gives information regarding the reserves needed to counterbalance the 95% of the positive imbalances.

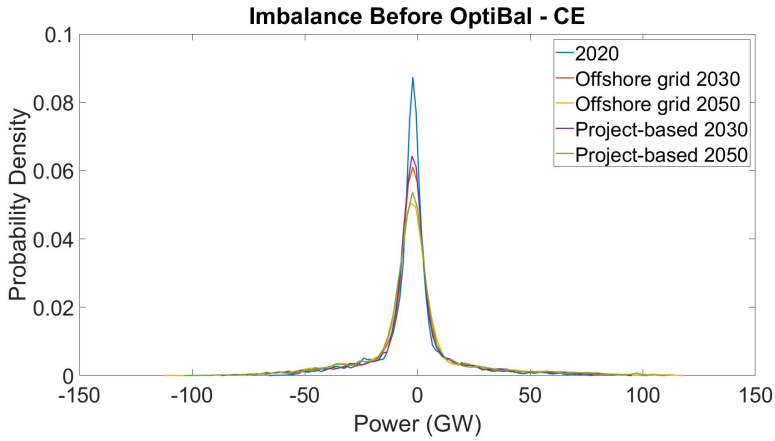


Figure (6.1) Probability density functions of Hour Ahead Imbalance (Hour Ahead forecast - Day Ahead dispatch) of Continental Europe synchronous area for each scenario and year.

From figure 6.1, it can be observed that balancing reserve requirement for CE (only considering the North Sea countries) does not change towards 2050. This is an important finding and can be attributed to the smoothening effect of large area on wind power variability. This demonstrates that neighbouring regions can support substantially for the balancing in each control area.

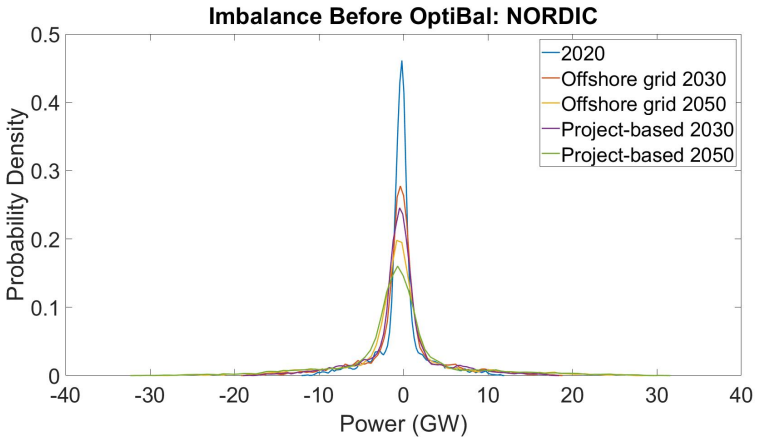


Figure (6.2) Probability density functions of Hour Ahead Imbalance (Hour Ahead forecast - Day Ahead dispatch) of Nordic synchronous area for each scenario and year.

However, for Nordic synchronous area, the balancing reserve requirements increase towards 2050. However, the increase is not substantial. It is also interesting to note the long tails of the probability density functions, depicting that very large imbalances can happen for very few hours of the year. In these hours, there might not be enough reserves available deploying automatic reserves.

The probability density of the imbalances occurred in DK1 and DK2 control areas are presented in figures 6.3 and 6.4 respectively. The volume of the imbalances appearing in the DK1 and DK2 control areas is increasing towards 2050 following the share of energy generated from wind. Thus, DK1 control area experiences larger imbalances in the Offshore grid scenario and DK2 in the Project-based scenario.

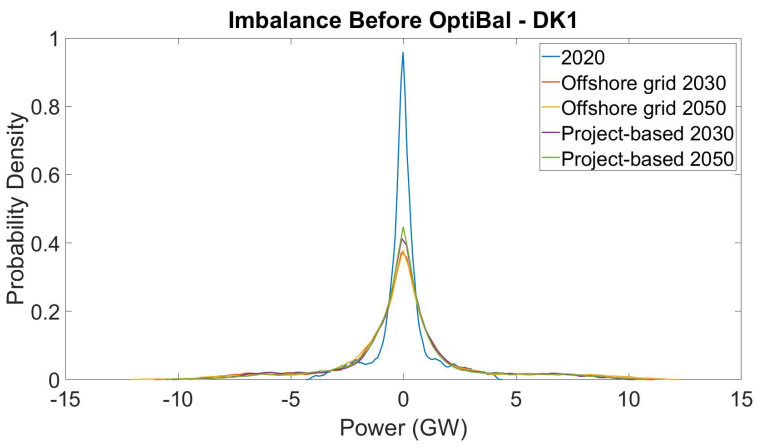


Figure (6.3) Probability density functions of Hour Ahead Imbalance (Hour Ahead forecast - Day Ahead dispatch) of DK1 control area for each scenario and year.

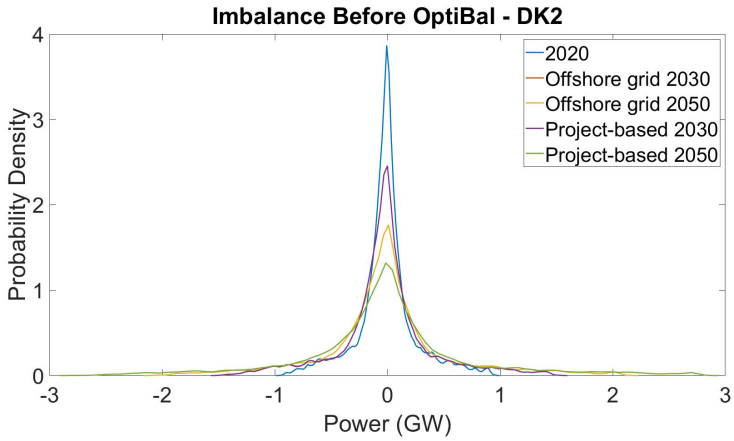


Figure (6.4) Probability density functions of Hour Ahead Imbalance (Hour Ahead forecast - Day Ahead dispatch) of DK2 control area for each scenario and year.

As mentioned, the tables 6.1 and 6.2 present the the $5^{th}$ and the $95^{th}$ percentile values of the input imbalances for some of the control areas simulated.

**p5 Value of Imbalance Before OptiBal (GW)**

| | | Offshore grid | | Project-based | |
|---|---|---|---|---|---|
| **Control Area** | **2020** | **2030** | **2050** | **2030** | **2050** |
| **BELGIUM** | -2.2 | -6.3 | -5.9 | -6.3 | -5.8 |
| **GERMANY** | -21.5 | -29.8 | -33.5 | -24.8 | -27.4 |
| **NETHERLANDS** | -3.3 | -3.2 | -3.4 | -8.5 | -11.5 |
| **NORWAY** | -1.4 | -5.9 | -6.3 | -5.8 | -8.0 |
| **SWEDEN** | -4.4 | -4.4 | -8.9 | -4.4 | -8.9 |
| **DK1** | -2.8 | -7.0 | -7.1 | -6.4 | -6.1 |
| **DK2** | -0.6 | -1.0 | -1.3 | -1.0 | -1.7 |

Table (6.1) The $5^{th}$ percentile value of the imbalance before OptiBal for each scenario and year.

**p95 Value of Imbalance Before OptiBal (GW)**

| | | Offshore grid | | Project-based | |
|---|---|---|---|---|---|
| **Control Area** | **2020** | **2030** | **2050** | **2030** | **2050** |
| **BELGIUM** | 2.1 | 6.4 | 6.4 | 6.4 | 6.4 |
| **GERMANY** | 30.7 | 38.4 | 49.4 | 36.1 | 42.6 |
| **NETHERLANDS** | 3.3 | 3.3 | 3.7 | 8.6 | 14.7 |
| **NORWAY** | 1.4 | 6.1 | 7.4 | 6.0 | 8.6 |
| **SWEDEN** | 5.1 | 5.1 | 9.6 | 5.1 | 9.6 |
| **DK1** | 3.0 | 7.6 | 8.4 | 7.0 | 7.3 |
| **DK2** | 0.6 | 1.0 | 1.5 | 1.0 | 2.0 |

Table (6.2) The $95^{th}$ percentile value of the imbalance before OptiBal for each scenario and year.

It can be observed from above figures and tables that hour-ahead imbalances in DK1 increase substantially from approximately ± 3GW in 2020 to ± 7-8GW by 2030 and 2050.

While, the hour-ahead imbalances in DK2 only increase little from ± 600 MW in 2020 to ± 1GW in 2030 to ± 2GW in 2050.

### 6.2.2 Prices – Balancing Cost

In this section, the cumulative probability distribution curves of the prices derived from the Intra Hour balancing market are presented for the control areas DK1 and DK2 in each scenario and year. The prices of the two Danish regions for up regulation are illustrated in figures 6.5 and 6.6. As shown in table 6.3, the average prices of all control areas increase from 2020 to 2030 and decrease from 2030 to 2050. This development is related to the $CO_2$ price assumptions and the penetration of VRE in the energy system. The fact that the use of fossil fuels is still considerable in 2030 and in the same time, the $CO_2$ price experiences a big increase (from 6 €/t $CO_2$ to 76.7 €/t $CO_2$) leads to increase of prices. This increase in prices can be seen in all the regions as shown in Tables 6.3 and 6.4.

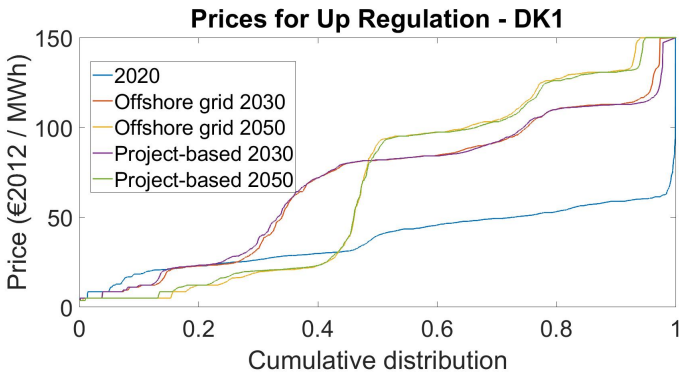


Figure (6.5) The cumulative probability curves (duration curves) for the electricity prices for up regulation in each scenario and year for the region DK1.

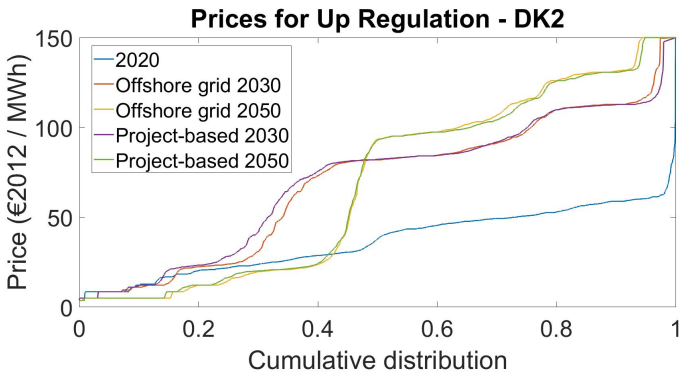


Figure (6.6) The cumulative probability curves (duration curves) for the electricity prices for up regulation in each scenario and year for the region DK2.

| Average Prices for Up Regulation ( €2012/MWh) | | | | | |
|---|---|---|---|---|---|
| | | Offshore grid | | Project-based | |
| **Control Areas** | **2020** | **2030** | **2050** | **2030** | **2050** |
| **GERMANY** | 40.1 | 75.9 | 73.2 | 75.7 | 73.0 |
| **NETHERLANDS** | 47.5 | 72.2 | 71.5 | 74.2 | 73.6 |
| **NORWAY** | 32.9 | 60.3 | 53.4 | 59.4 | 55.4 |
| **SWEDEN** | 37.9 | 63.4 | 74.5 | 63.3 | 73.4 |
| **DK1** | 37.9 | 69.5 | 68.2 | 69.6 | 67.9 |
| **DK2** | 36.6 | 69.2 | 68.8 | 70.4 | 68.6 |

Table (6.3) The average price for up regulation for each scenario and year

Next, the cumulative probability functions of the price for down regulation in DK1 and DK2 are illustrated in figures 6.7 and 6.8 respectively. Moreover, the table 6.4 presents the average down regulation price. Again, the prices of all control areas are expanding from 2020 to 2030 as the $CO_2$ price increases and decreasing from 2030 to 2050 following the fossil fuel usage.

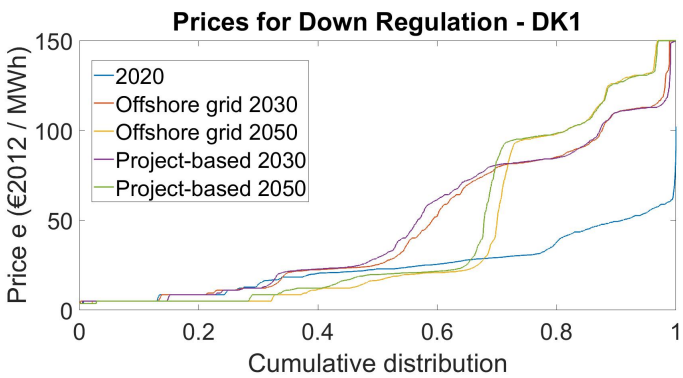


Figure (6.7) The cumulative probability curves for the electricity prices for down regulation in each scenario and year for the region DK1

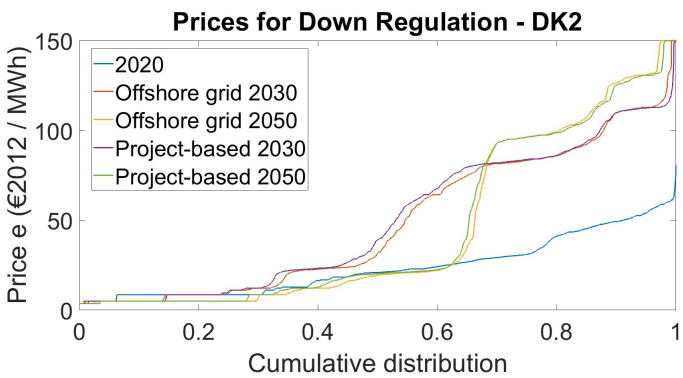


Figure (6.8) The cumulative probability curves for the electricity prices for down regulation in each scenario and year for the region DK2

| Average Prices Down Regulation ( €2012/MWh) | | | | | |
|---|---|---|---|---|---|
| | | Offshore grid | | Project-based | |
| **Control Areas** | **2020** | **2030** | **2050** | **2030** | **2050** |
| **GERMANY** | 21.1 | 46.5 | 40.3 | 47.9 | 41.2 |
| **NETHERLANDS** | 35.5 | 47.7 | 39.2 | 51.0 | 44.3 |
| **NORWAY** | 36.2 | 54.2 | 49.5 | 54.7 | 49.8 |
| **SWEDEN** | 29.9 | 47.2 | 47.3 | 47.0 | 47.5 |
| **DK1** | 24.5 | 46.6 | 41.7 | 47.6 | 43.8 |
| **DK2** | 23.7 | 48.5 | 44.9 | 49.6 | 45.4 |

Table (6.4) The average price for down regulation for each scenario and year

### 6.2.3 Reserve Deployed

As explained during the Optibal optimization, hour-ahead wind generation forecast simulations (more accurate than day-ahead) are taken into consideration and thus the Day Ahead dispatch schedule is changed. The generators participating in the Intra-Hour balancing are regulating their dispatch level up or down depending on the instantaneous forecast error. The optimization algorithm considers the ramping capabilities of each technology as well as its costs for regulating its generation level in order to choose which generator should change its generation. The figures 6.9 and 6.10 show the activated balancing reserves for up regulation divided into the technology type for the Continental Europe and Nordic synchronous areas. As shown, the technology that is mainly used in the balancing alters between the two synchronous areas and that is due to the differences in the installed capacities mix. In principal, in Continental Europe, the negative imbalances are mainly counteracted from technologies that use Natural gas as their fuel. The highest share of activated reserves from Natural gas technologies in respect to the aggregated balancing reserves is 93.5% and occurs in the Offshore grid scenario in the year 2030. In the other hand, the Nordic synchronous area is depending more on hydro technologies for cancelling out the negative imbalances. The highest share of reserves from Hydro technologies in balancing is 90.2% and is recorded in the year 2020. Wind technologies are also used for up-regulation if they are being curtailed in the day-ahead schedule.

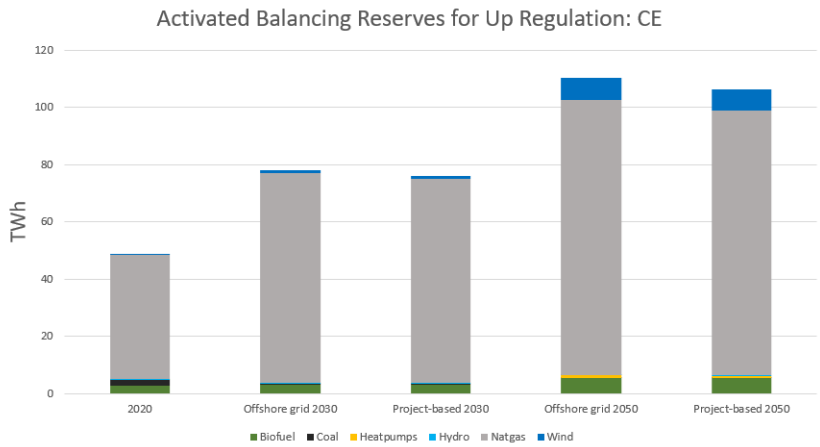


Figure (6.9) Activated balancing reserves for up regulation in CE synchronous area per scenario,year and technology type.

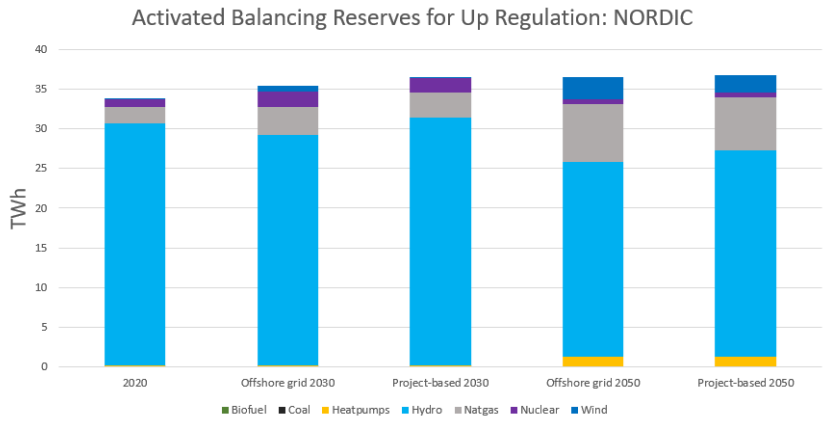


Figure (6.10) Activated balancing reserves for up regulation in Nordic synchronous area per scenario,year and technology type.

The figures 6.11 and 6.12 depict the activation of balancing reserves for down regulation in Continental Europe and Nordic synchronous areas respectively. In Continental Europe in the year 2020, natural gas and coal technologies contribute in balancing positive imbalances with 46.2% and 26.5% of the aggregated activated reserves respectively. As coal technologies are decommissioning towards 2050, the reserves mix is changing and consists mainly of Natural gas and hydro technologies. In Nordic synchronous area, natural gas technologies are dominating in the contribution for down regulation in all scenarios and years.

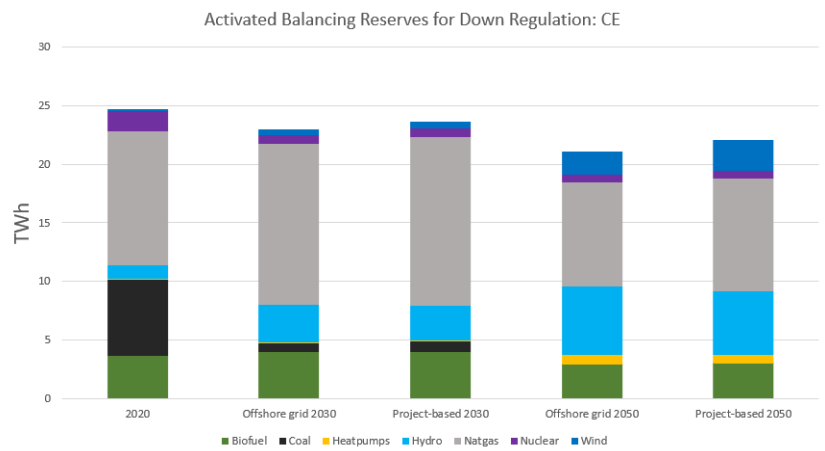


Figure (6.11) Activated balancing reserves for down regulation in CE synchronous area per scenario, year and technology type.

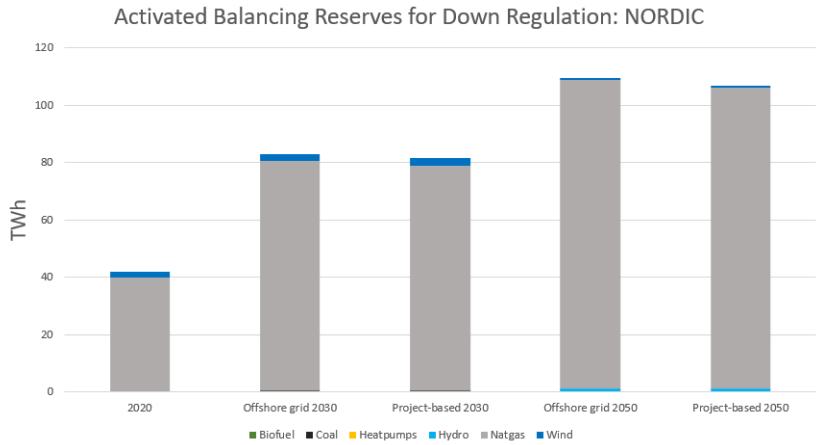


Figure (6.12) Activated balancing reserves for down regulation in Nordic synchronous area per scenario, year and technology type.

The activated balancing reserves for up and down regulation divided into the technology type for the Danish control area DK1 are shown in figures 6.13 and 6.14 respectively. Furthermore, the up and down regulation of the interconnection lines during the Intra Hour market for balancing purposes is calculated and presented in figure 6.15.

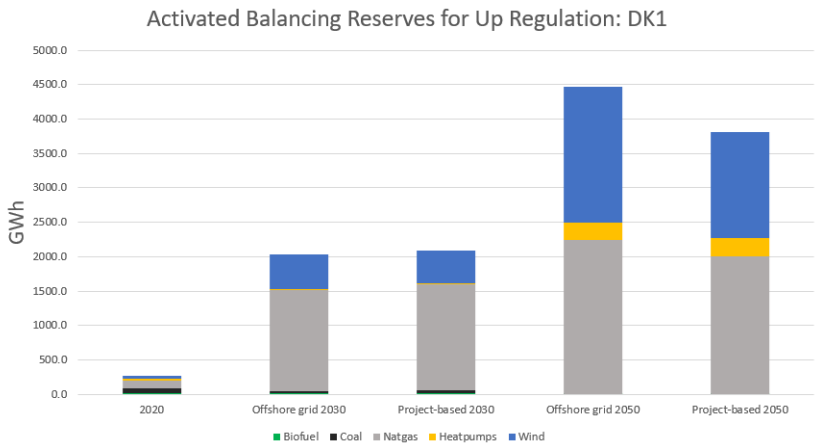


Figure (6.13) Activated balancing reserves for up regulation in DK1 control area per scenario,year and technology type.

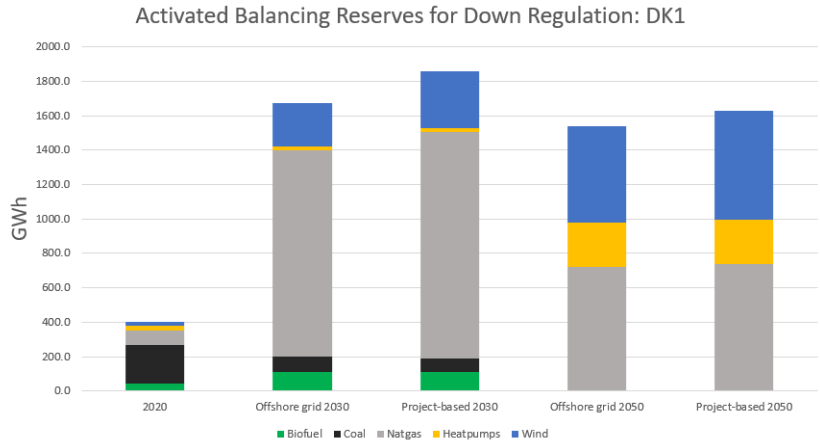


Figure (6.14) Activated balancing reserves for down regulation in DK1 control area per scenario,year and technology type.

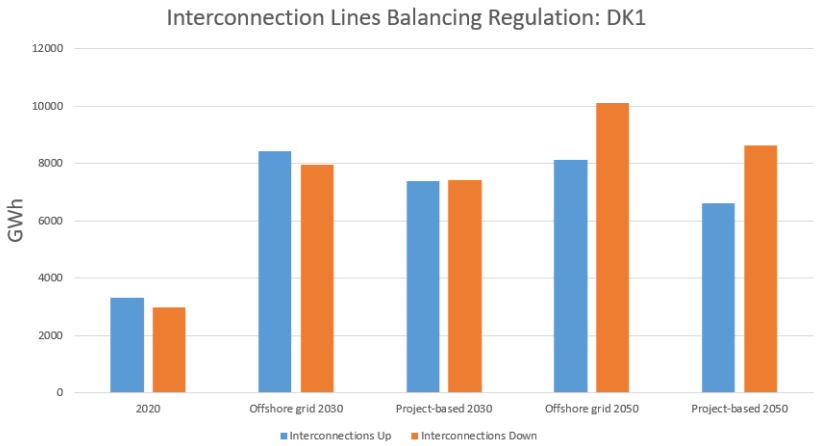


Figure (6.15) Activated interconnection lines for balancing regulation in DK1 control area per scenario,year and technology type.

Based on these three graphs, it is obvious that DK1 is heavily dependent on its interconnection lines for the Intra Hour balancing. Moreover,it can be observed that technologies using Natural gas are dominating in terms of up and down activated balancing reserves until 2030. In contrary, in 2050 for both project-based and offshore grid scenario the contribution of wind technologies for up regulation during balancing is 40% and 44% respectively. Regarding the balancing reserves activated for down regulation the wind technologies in project-based and in offshore grid scenario contributed for 37% and 39% respectively.

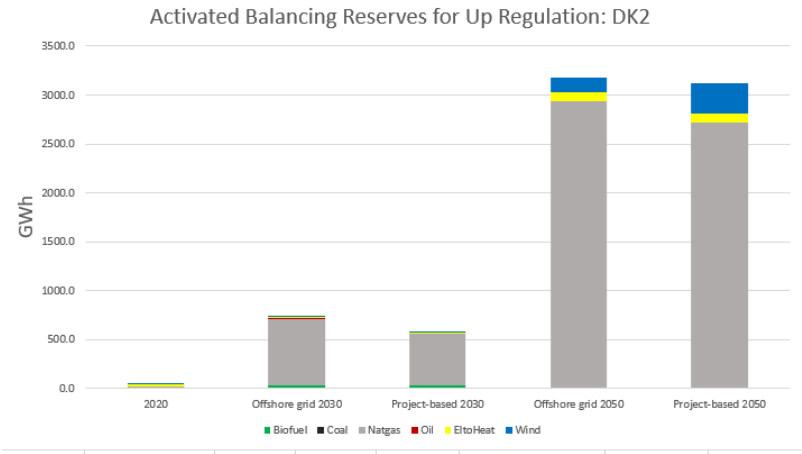


Figure (6.16) Activated balancing reserves for up regulation in DK2 control area per scenario,year and technology type.

The activated balancing reserves for up and down regulation in DK2 are shown in figures 6.16 and 6.17 respectively. The up and down regulation of the interconnection lines connected to DK2 are presented in figure 6.18.

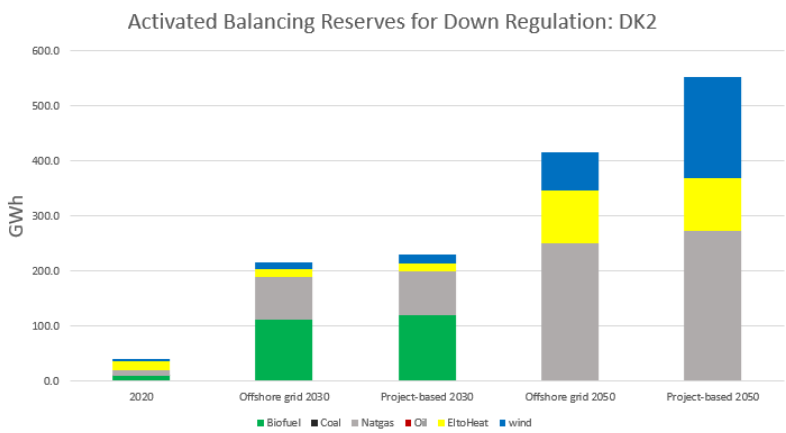


Figure (6.17) Activated balancing reserves for down regulation in DK2 control area per scenario,year and technology type.

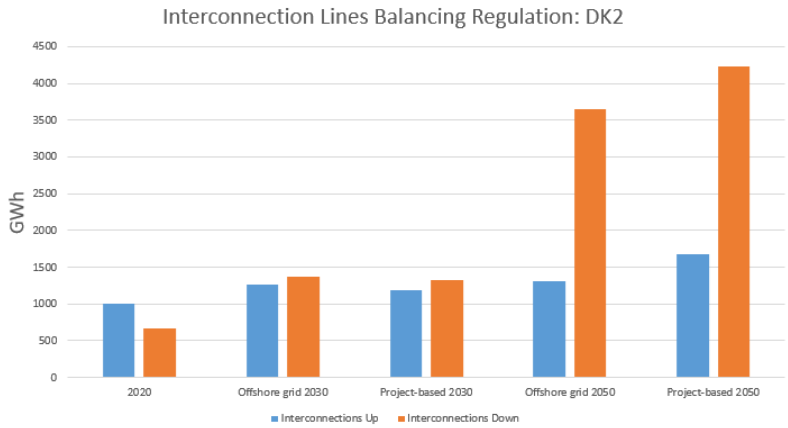


Figure (6.18) Activated interconnection lines for balancing regulation in DK2 control area per scenario,year and technology type.

The results concerning the control area DK2 prove once more the dominant role of interconnection lines in Intra Hour balancing. Especially in the simulation of the year 2020, most of the regulation is coming from the neighboring control areas. Regarding the up regulation of domestic generators in DK2 for 2030 and 2050 in both scenarios the majority is coming from technologies using Natural Gas. In contrary, in 2030 for for both scenarios, the down regulation reserves deployed were using Biofuel by 52 %. The support provided from the wind for down regulation in the year 2050 for project based and offshore grid scenario is 33% and 17% respectively.

### 6.2.4 Hours with inadequate balancing reserves

During the OptiBal optimization procedure there are instants where the balancing reserves are not enough to cover the input imbalance due to the lack of domestic reserves and the constrains of the interconnection lines. These limitations are expressed in the problem of balancing with two forms depending on sign of the imbalance. In cases of positive imbalance, if there are not enough reserves wind generation will be curtailed. In cases of negative imbalance, the system lacks generation and that leads to infeasibilities in the optimization process. The volume of the imbalances that couldn't be covered was quantified for each scenario and year in the table 6.5.

**Volume of missing reserves (GWh)**

| | | Offshore grid | | Project-based | |
|---|---|---|---|---|---|
| **Control Area** | **2020** | **2030** | **2050** | **2030** | **2050** |
| **DK1** | 0.0 | 0.0 | 0.0 | 0.0 | 0.0 |
| **DK2** | 0.0 | 0.0 | 0.0 | 0.0 | 0.0 |

Table (6.5) The volume of missing balancing reserves in OptiBal in Gwh for each scenario and year

The total hours where there are not enough balancing reserves to be activated are calculated and presented in table 6.6.

**Hours with no Balancing Reserves**

| | | Offshore grid | | Project-based | |
|---|---|---|---|---|---|
| **Control & Synchronous Areas** | **2020** | **2030** | **2050** | **2030** | **2050** |
| **DK1** | 0.0 | 0.0 | 0.0 | 0.0 | 0.0 |
| **DK2** | 0.0 | 0.0 | 0.0 | 0.0 | 0.0 |

Table (6.6) The hours with no balancing reserves for each scenario and year.

As explained in section 5.2.4, a ”back-up” installed capacity was added in each region in order its demand for electricity to be always covered during the Day Ahead market. In OptiBal, an ”artificial” constraint was added limiting the maximum back-up power that could be used in each region with the one used in DA. In case of Sweden and Norway, the ”back-up” power was barely used in the DA and thus it could not be dispatched in IH. This is the reason for the large volume of missing reserves in these two regions.

# Chapter 7

# Area Control- Dynamic Model

In this chapter, the Area Control-Dynamic models simulating the activation of automatic reserves and the frequency deviation for both Continental Europe and the Nordic synchronous areas are presented. In addition the aforementioned studied scenarios are compared in terms of the input imbalance, frequency deviation, FCR and FRR deployment and the instantaneous inertia of the system. The results are only shown for a few regions for illustrative purposes and to limit the size of this report.

## 7.1 Modelling

As described before, close to real time and ultimately in real time the imbalance between the electricity demand and generation determines the system frequency which is crucial for system stability. The frequency control methodology depends on both the physical and organisational characteristics of the particular synchronous area and thus differs among different synchronous areas of ENTSO-E [10], [11]. Although the European framework for integration of the balancing markets promotes harmonization of the Balancing services among the Balancing Service Providers (BSPs) each TSO may create and use specific products. The development of these specific products is allowed when by utilizing the standard products alone it can be proved that a) they cannot ensure the operational security, b) they are insufficient to maintain the system balance or c) there are balancing resources that are not able to participate in the balancing market through standard products [12].

TSOs have the responsibility of maintaining the operational security within the defined limits by utilizing manual and automatic reserves in mainly three balancing processes. The balancing products used in areas of ENTSO-E and the time scale of their deployment since an imbalance occurs are shown in figure 7.1.

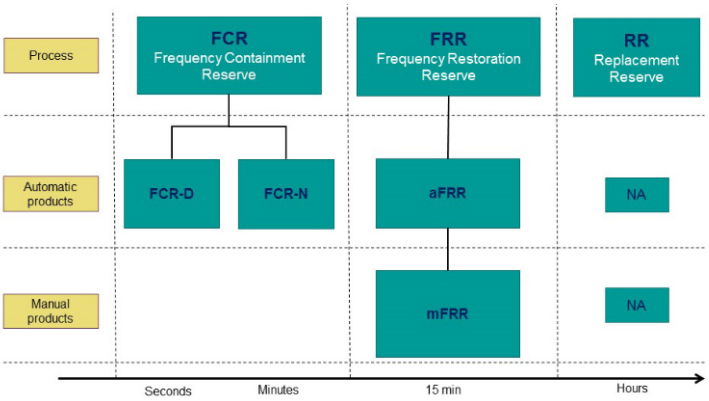


Figure (7.1) The chronology of the different frequency control processes in a synchronous area and its control areas as well as their reserves products. [13].

As shown, the Frequency Containment Reserves (FCR) are used seconds or minutes after the occurrence of the imbalance for the containment of frequency. The Frequency Restoration Reserves (FRR) are utilized around 15 minutes after the event for returning the frequency to its normal range (49.9 - 50.1 Hz) and to release FCR already deployed back into use. Lastly, the Replacement Reserves (RR) release activated FRR back to a state of readiness for use to counteract new imbalances [13].

### 7.1.1 Dynamic Modelling of Nordic System

In the Nordic system (Finland, Sweden, Norway and East Denmark), the obligations for maintaining reserves have been agreed in System Operation Agreement between the Nordic Transmission System Operators (TSOs). The balancing reserve process that are used in the Nordic synchronous area are the Frequency Containment Process (FCP) and the Frequency Restoration process (FRP). The balancing reserves products defined in the System Operation Agreement are namely the FCR-D, FCR-N , aFRR and mFRR.

The Frequency Containment Reserve for Normal operation (FCR-N) product is acting as a primary frequency control reserve and is used to balance the system within normal frequency band (49.9 - 50.1 Hz). In total, 600 MW of aggregated FCR-N are constantly maintained inside the Nordic area [13]. Thus, the bias factor of the FCR-N is calculated as $\frac{600}{0.1} = 6000[MW/Hz]$

The Frequency Containment Reserve for Disturbances (FCR-D) is also acting as a primary frequency control reserve. It is used to control the steady state frequency deviations from exceeding 0.5 Hz (49.5 - 50.5 Hz)in case of a disturbance such as the disconnection of a large production unit. In other words, the paid FCR-D should be activated within 0.4 Hz (49.9−49.5). The aggregated FCR-D available in the Nordic system is assumed in this report 1200 MW. Thus, the bias factor of the FCR-D is calculated as $\frac{1200}{0.4} = 3000[MW/Hz]$

As mentioned, the Frequency Restoration Reserve is acting as a secondary frequency control reserve and is separated into automatic (aFRR) and manual (mFRR). Due to the deteriorating frequency quality in the Nordic synchronous power system, the aFRR were introduced in 2013 as a companion to the existing mFRR. Advantages of using aFRR compared to mFRR is the obvious faster response and the fact that it is capable of being based

on a merit order and taking into account the congestion in the grid.

Even though FCR-N, FCR-D and aFRR are automatic they present one more fundamental difference. FCR-N and FCR-D are controlled locally and in the other hand the aFRR is controlled centrally. Having in mind the aforementioned characteristics the Nordic synchronous area, the Area Control-Dynamic Model is developed as shown in figure 7.2.

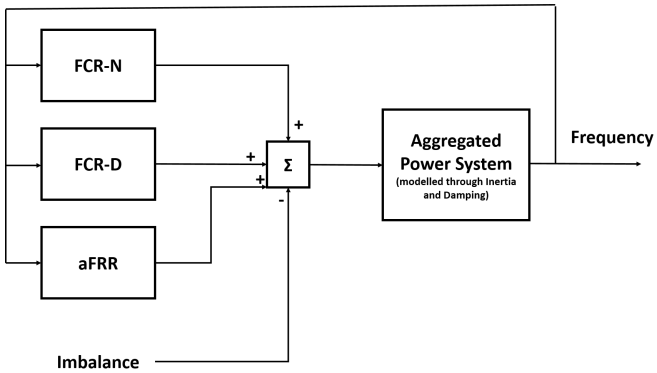


Figure (7.2) The Area Control-Dynamic Model of Nordic synchronous area

Detailed modelling of FCR-N, FCR-D and aFRR for Nordic network can be found in [14].

### 7.1.2 Dynamic Modelling of Continental Europe

Most of the times, large synchronous areas such as Continental Europe use a multi-tiered approach to frequency control [15]. First, the frequency containment is done locally by proportional control in order to ensure the avoidance of power oscillations in an abnormal operational state. Next, the frequency restoration is taking place in order the system to return to its pre-disturbance state. The frequency restoration, through Automatic Generation Control (AGC) or Load-Frequency Control (LFC), is done automatically and has proportional-integral control (or only integral control) characteristics. Furthermore, decentralised feedback implemented by each control area to respond to the local imbalance, contributes to the overall balance in the synchronous area. Based on the features and requirements of the state-of-the-art Continental Europe frequency control, the Area Control-Dynamic Model for Continental Europe is developed as illustrated in figure 7.3.

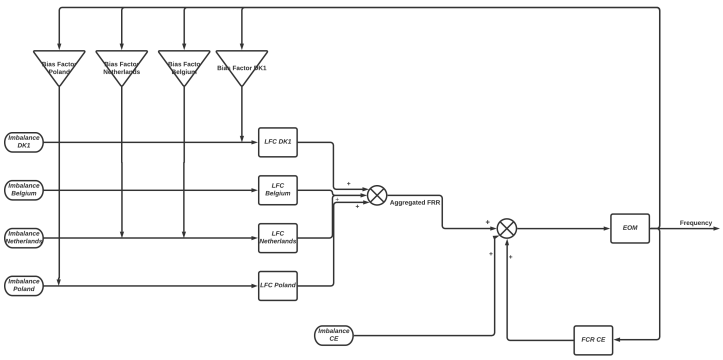


Figure (7.3) The Area Control-Dynamic Model of Continental Europe

As shown, the model includes again primary and secondary frequency control but in contrast with the Nordic synchronous area the primary is consisted only from one reserve product called FCR. The deployment of FCR in Continental Europe is considered to come only from thermal power units which are controlled centrally. The simulation model of FCR of Continental Europe is identical with the one presented in figure **??**

The secondary frequency control consists from automatic (aFRR) and manual (mFRR) Frequency Restoration Reserves. The aFRR is considered to be deployed by automatic LFC. The LFC control is modelled with an anti-windup PI controller together with measurement filter as shown in figure 7.4.

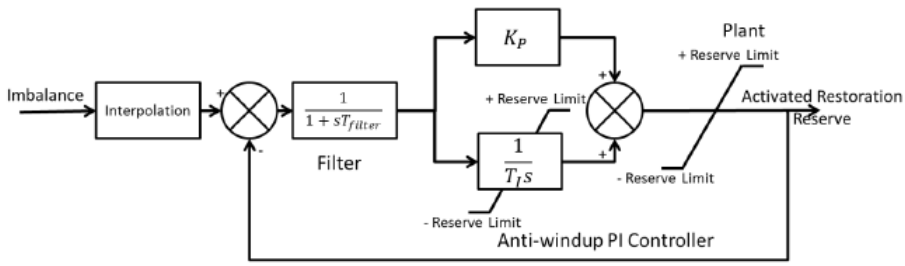


Figure (7.4) Model of the frequency restoration process (LFC) in Continental Europe.

### 7.1.3 Dimensioning of aFRR

The methodologies for dimensioning of aFRR as defined in UCTE's operation handbook differ among the control areas based on different operational needs [16]. The characteristics and patterns of generation and demand (including BRP and forecast qualities) of a control area determine the methodology based on which the available aFRR of the specific are calculated. In this report, the Probabilistic Risk Management Sizing Approach was used. According to that approach the minimum value for the sum of aFRR capacity and RR capacity is defined as the 99% quantile of the yearly imbalance [17]. As explained, the calculation of the aFRR in case of Continental Europe is done in control area level but for the Nordic system centrally by considering the aggregated imbalance. The available aFRR for each control area per scenario and year are presented in table 7.1. It can be observed the required volumes of aFRR requirement in 2030 and 2050 grow 3 to 4 times of the 2020 value. It should be noted that currently, aFRR dimensioning in Denmark may not necessarily follow probabilistic method. However, in future scenarios it is advisable to use probabilistic method to cater to imbalances caused by VRE forecast error. Another important point to note that, all the frequency reserves are also allocated to mitigate the imbalances due to unforeseen disturbances. In case the frequency reserves are eroded in mitigation of VRE forecast error, power system security can be compromised.

| aFRR available (GW) | | | | | |
|---|---|---|---|---|---|
| | | Offshore grid | | Project-based | |
| **Control & Synchronous Areas** | **2020** | **2030** | **2050** | **2030** | **2050** |
| **BELGIUM** | 0.5 | 1.9 | 1.9 | 1.9 | 1.9 |
| **GERMANY** | 3.1 | 4.3 | 5.7 | 3.5 | 4.6 |
| **NETHERLANDS** | 0.5 | 0.5 | 0.5 | 1.7 | 2.9 |
| **DK1** | 0.4 | 1.3 | 1.5 | 1.1 | 1.1 |
| **Nordic** | 0.5 | 1.4 | 1.6 | 2.1 | 3.5 |

Table (7.1) The available automatic Frequency Restoration Reserves (aFRR) for each scenario and year.

## 7.2 Comparison among scenarios

### 7.2.1 Analysis of Input Imbalance

In this section, the Real Time imbalances viewed as input from the Area Control model are presented for each scenario and year. Figure 7.5 and 7.6 depict the imbalance after the Intra Hour balancing in DK1 and DK2 control area respectively. As expected, the probability density functions of the imbalances gets wider towards 2050 meaning higher imbalances. This demonstrates that the imbalance increases substantially by 2030. However, the imbalance is practically same for both the project based and offshore grid scenarios for DK1 control area. However, for DK2 control area imbalance for 2050 scenario is more than that of 2030 scenario. Similar to DK1, project based scenario and offshore grid scenarios have almost same values of imbalance.

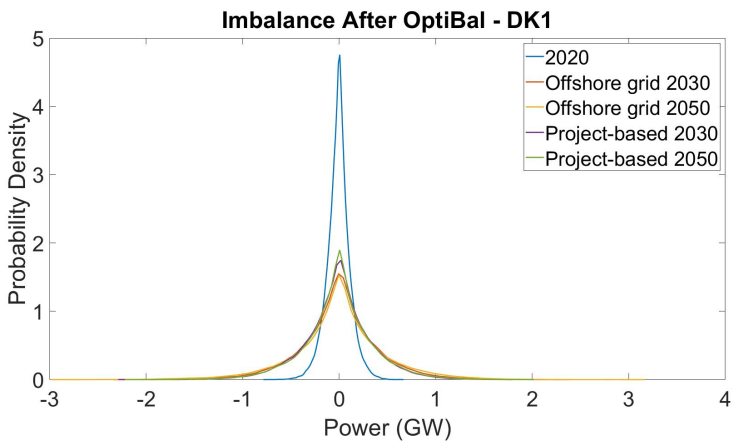


Figure (7.5) Probability density functions of Real Time Imbalance (Real Time available wind - Hour Ahead dispatch) of DK1 control area for each scenario and year.

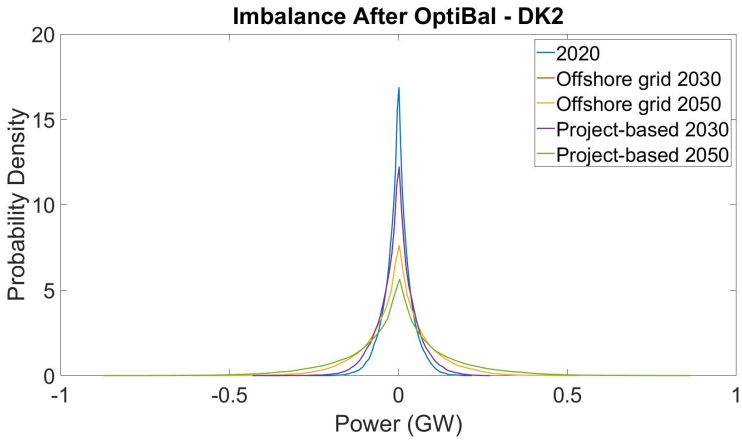


Figure (7.6) Probability density functions of Real Time Imbalance (Real Time available wind - Hour Ahead dispatch) of DK2 control area for each scenario and year.

Since the frequency control is done in synchronous area level, the aggregated Real Time imbalances of Continental Europe and Nordic system for each scenario and year are illustrated in figure 7.7 and 7.8 respectively. Continental Europe as a much larger system than the Nordic experiences much greater imbalances that can reach up to $10GW$ towards 2050. It is worth mentioning, that the aggregated imbalance in the Nordic synchronous area in the project based scenario 2030 is comparable with the one calculated in the scenario of offshore grid 2050.

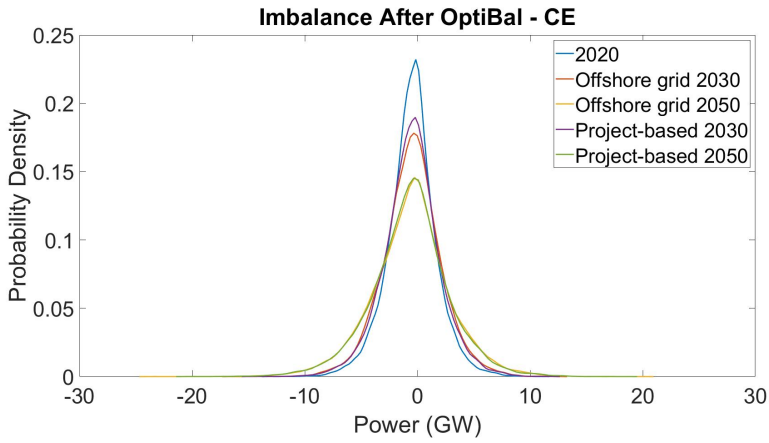


Figure (7.7) Probability density functions of Real Time Imbalance (Real Time available wind - Hour Ahead dispatch) of Continental Europe synchronous area for each scenario and year.

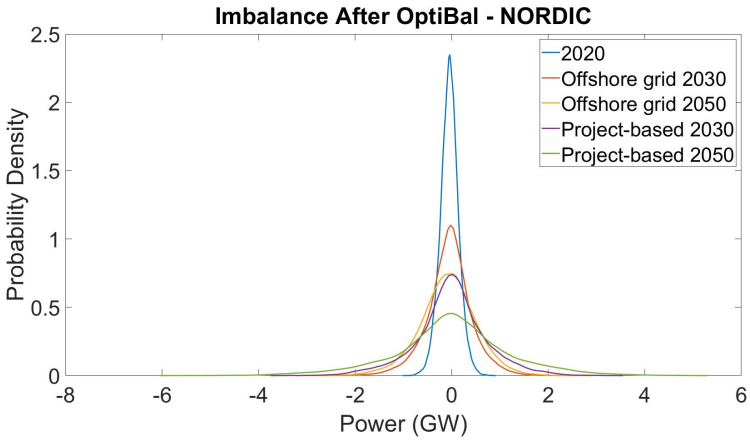


Figure (7.8) Probability density of Real Time Imbalance (Real Time available wind - Hour Ahead dispatch) of Nordic synchronous area for each scenario and year.

The $5^{th}$ and $95^{th}$ percentiles of the Real Time imbalances for different control areas of the model are presented in tables 7.2 and 7.3 respectively.

**p5 Value of Imbalance After OptiBal (GW)**

| | | Offshore grid | | Project-based | |
|---|---|---|---|---|---|
| **Control & Synchronous Areas** | **2020** | **2030** | **2050** | **2030** | **2050** |
| **BELGIUM** | -0.4 | -1.4 | -1.4 | -1.4 | -1.3 |
| **GERMANY** | -2.3 | -3.1 | -4.0 | -2.6 | -3.4 |
| **NETHERLANDS** | -0.4 | -0.4 | -0.4 | -1.2 | -2.1 |
| **NORWAY** | -0.1 | -1.0 | -1.0 | -1.6 | -2.5 |
| **SWEDEN** | -0.3 | -0.3 | -0.7 | -0.3 | -0.7 |
| **DK1** | -0.3 | -0.9 | -1.1 | -0.8 | -0.8 |
| **DK2** | -0.1 | -0.1 | -0.2 | -0.1 | -0.3 |
| **CE** | -4.8 | -5.6 | -7.7 | -5.5 | -7.7 |
| **NORDIC** | -0.4 | -1.0 | -1.3 | -1.7 | -2.6 |

Table (7.2) The $5^{th}$ percentile value of the imbalance after OptiBal for each scenario and year.

**p95 Value of Imbalance After OptiBal (GW)**

| Control & Synchronous Areas | 2020 | Offshore grid 2030 | Offshore grid 2050 | Project-based 2030 | Project-based 2050 |
|---|---|---|---|---|---|
| **BELGIUM** | 0.4 | 1.3 | 1.3 | 1.3 | 1.3 |
| **GERMANY** | 2.0 | 2.9 | 3.9 | 2.3 | 3.0 |
| **NETHERLANDS** | 0.3 | 0.3 | 0.4 | 1.2 | 2.0 |
| **NORWAY** | 0.1 | 0.9 | 1.0 | 1.6 | 2.5 |
| **SWEDEN** | 0.3 | 0.3 | 0.6 | 0.3 | 0.6 |
| **DK1** | 0.2 | 0.9 | 1.0 | 0.7 | 0.8 |
| **DK2** | 0.1 | 0.1 | 0.2 | 0.1 | 0.3 |
| **CE** | 4.3 | 5.1 | 6.9 | 5 | 6.7 |
| **NORDIC** | 0.4 | 0.9 | 1.1 | 1.5 | 2.5 |

Table (7.3) The $95^{th}$ percentile value of the imbalance after OptiBal for each scenario and year.

It can be noticed that the imbalance in DK1 increases substantially from 2020 (-0.3,0.2 GW) to 2030 scenario (±0.9GW), while the increase from 2030 to 2050 (-1.1,1 GW) is not that much. Offshore grid scenario has around 100 to 200 MW more imbalance pertaining to slightly more installation of wind power in offshore grid scenario as compared to project based scenario. The increase in imbalance for DK2 network is around 100 to 200 MW compared to 2020 for 2050 scenario. The imbalances are same in 2030 scenario as that of 2020 scenario.

It is very important to see that Offshore grid scenario observes much less real time imbalance as compared to Project based scenario for Nordic network.

### 7.2.2 Power System Inertia

As mentioned in the introduction, the VRE penetration challenges the power system's adequacy by decreasing the aggregated inertia of the system. The physical significance of inertia is that equals the stored kinetic energy in the rotating masses of the power system (i.e synchronous generators). This energy is inherently exchanged with the system during disturbances holding down the frequency fluctuations. Renewable generation units, such as solar PV and wind generators are decoupled from the grid through power electronic converters and thus provide no inertia making the frequency of the system more prone to faster change in frequency following an imbalance.

The inertia provided is technology specific and is an inherent attribute of each technology. The inertia constant H is used to quantify the inertia and it is expressed in seconds as it denotes the time from a generator in order to provide its rated power solely using the kinetic energy stored in the rotating mass of its governor. The inertia constant assumed in this report for the calculation of the power system inertia are presented in table 7.4.

| Technology Type | Inertia Constant (s) |
|---|---|
| Combined Cycle | 8 |
| Steam Turbine | 6.09 |
| Gas Turbine | 8.28 |
| Internal Combustion Engine | 5.29 |
| Hydro Technologies | 2.4 |
| Nuclear | 4.07 |
| VRE | 0 |

Table (7.4) Inertia constant assumptions for different technologies

Based on these parameters, the inertia of the system can be calculated as $H_{sys} = \frac{\sum_i H_i \cdot S_i}{S_{sys}}$ , where $S_i$ is the the rated power of the machine and i the online machines for a given time-step. The probability densities of the system inertia in synchronous areas CE and Nordic are depicted in figures 7.9 and 7.10 respectively for each scenario and year.

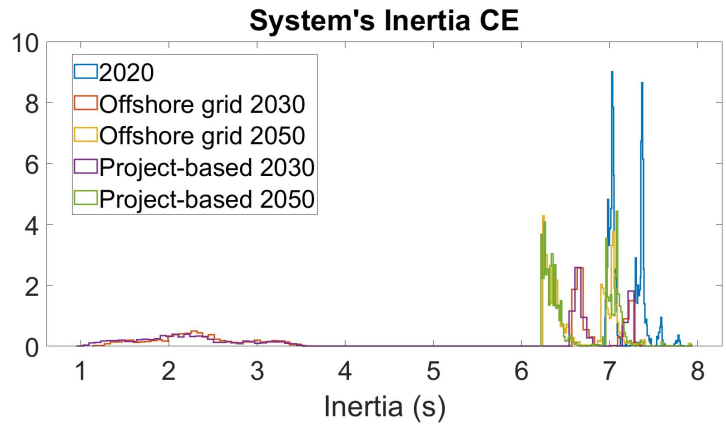


Figure (7.9) Normalised Histogram of system inertia in Continental Europe synchronous area for each scenario and year.

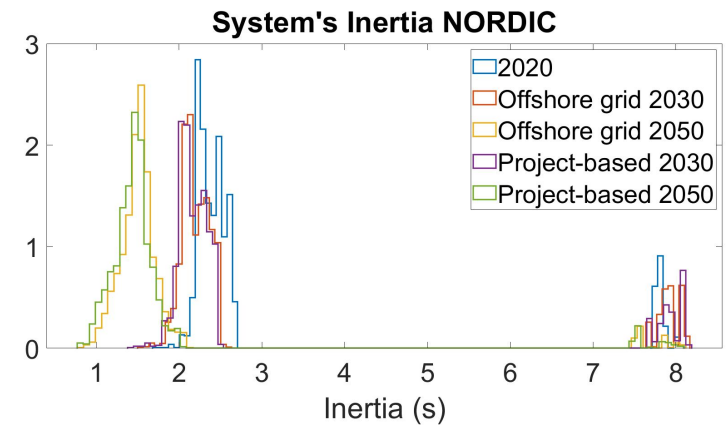


Figure (7.10) Normalised Histogram of system inertia in Nordic synchronous area for each scenario and year.

It can be observed that the inertia in CE synchronous area although reduces from 2020 value is not alarming even for 2050 scenario. Although there might be few hours possible

where the inertia might go low. However, for Nordic network, the inertia is highly impacted in 2030 and 2050 scenario. Although, these inertia calculation can be pessimistic because the inertia of loads and other components like synchronous condensers are not taken into account.

### 7.2.3 Frequency

As explained, by simulating the deployment of the automatic reserves it is possible to observe the frequency variations along the year for each scenario. The probability density functions of the electric frequency in both synchronous areas CE and Nordic for each scenario and year are presented in figures 7.11 and 7.12 respectively. Next, the table 7.5 shows the number of hours per year in which the frequency is outside from the nominal range where that the nominal frequency range is defined as $50 \pm 50mHz$ for CE and $\pm 100mHz$ for Nordic network. As shown, from both the graphs and the table that the frequency experiences larger variations despite the fact that the FRR are always dimensioned in way that their capacity equals the 99% quantile of the yearly imbalance. The reason of this happening is that the variations of the imbalance are also increasing towards 2050 making it more difficult for the automatic reserves to counteract in terms of speed of activation. It should be noted that Nordic network has more impact in future scenarios as compared to 2020 scenario. While for CE network, the frequency beyond the nominal value is same as in 2020 scenario. Project based and offshore grid scenarios do not have big differences.

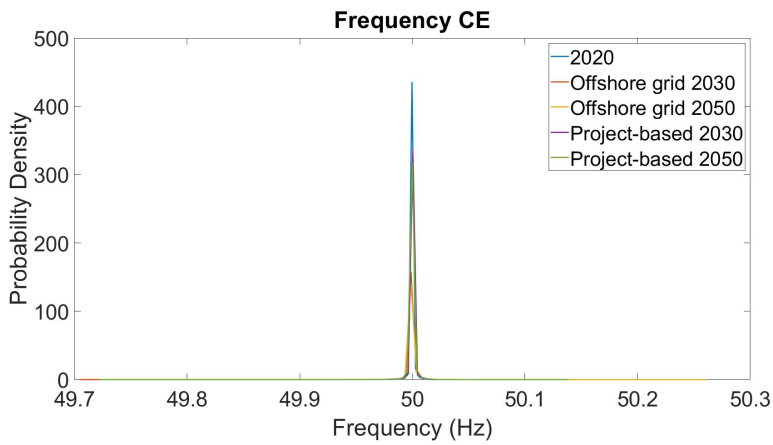


Figure (7.11) Probability density of Real Time frequency (Hz) in CE synchronous area for each scenario and year.

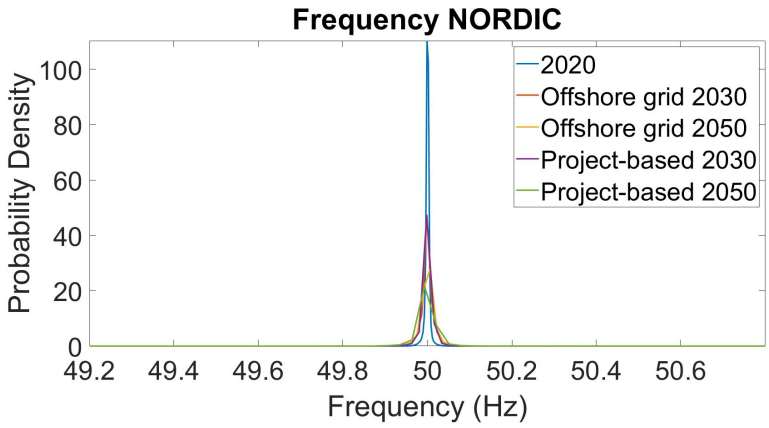


Figure (7.12) Probability density of Real Time frequency (Hz) in Nordic synchronous area for each scenario and year.

| Scenarios | CE | Nordic |
|---|---|---|
| **2020** | 12.5 | 0.9 |
| **Project-based 2030** | 16.8 | 13.6 |
| **Offshore grid 2030** | 16.8 | 16.8 |
| **Project-based 2050** | 23.4 | 35.6 |
| **Offshore grid 2050** | 31.2 | 22.0 |

Table (7.5) Hours outside Nominal Freqeuncy range (CE: $\pm 50mHz$, Nordic: $\pm 100mHz$) for each scenario and year

### 7.2.4 FCR activation

In this section, the activation of reserves during the frequency containment process in CE and Nordic synchronous areas for each scenario and year are illustrated. The probability density functions of the FCR deployment in CE and of the FCR-N in Nordic is depicted in figure 7.13 and 7.14 respectively. As shown, in both synchronous areas the frequency containment for normal operation are reaching their limits only for a very few instances per year. However, FCR are being activated quite many hours. This is especially challenging since FCR are currently dimensioned to mitigate large (N-1) disturbances. If VRE forecast error imbalances use up the FCR, the system security is highly compromised. This is especially observed in Nordic network. It can be advisable to allocate additional FCR in future to handle VRE based imbalances. Currently, FCR in CE is dimensioned as 3000 MW. It can be seen from the results that approximately 30 to 60 MW of that reserve is used to balance the forecast error. Whereas, Nordic network has FCR-N of around 600 MW. In 2050 scenario, around 200 MW of FCR-N is utilized to minimize the imbalance as compared to 50 MW in 2020 scenario. It shows that in future more reserves might be required to be allocated keeping allowance for other kind of uncertainties like loads and other variable generations.

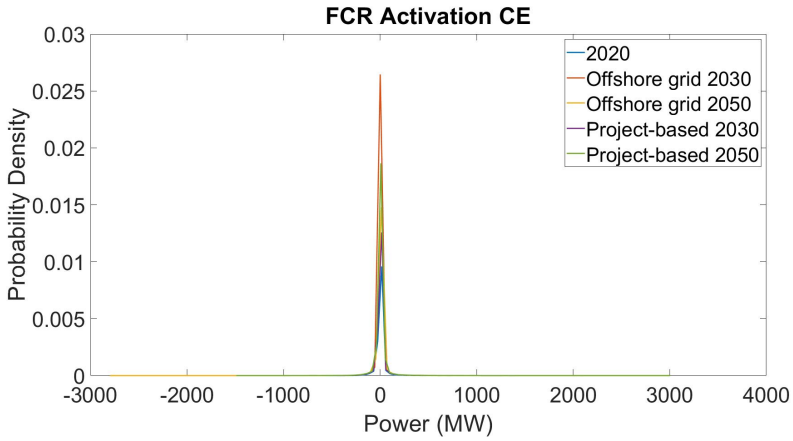


Figure (7.13) Probability density function of FCR activation in Continental Europe for each scenario and year.

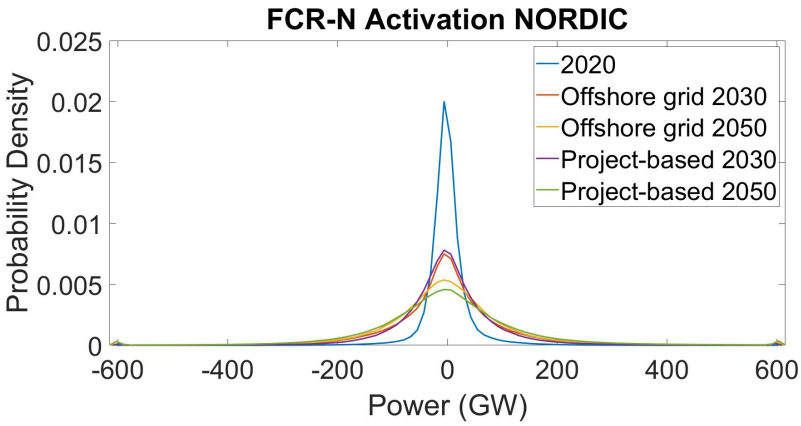


Figure (7.14) Probability density function of FCR-N activation in Nordic system for each scenario and year.

**p5 Value of FCR Activation (MW)**

| | | Offshore grid | | Project-based | |
|---|---|---|---|---|---|
| **Synchronous Areas** | **2020** | **2030** | **2050** | **2030** | **2050** |
| CE | -33.5 | -44.8 | -52.3 | -43.7 | -55.4 |
| NORDIC | -47.7 | -164.4 | -176.5 | -133.6 | -209.4 |

Table (7.6)

**p95 Value of FCR Activation (MW)**

| | | Offshore grid | | Project-based | |
|---|---|---|---|---|---|
| **Synchronous Areas** | **2020** | **2030** | **2050** | **2030** | **2050** |
| CE | 34.5 | 45.8 | 52.9 | 44.7 | 59.3 |
| NORDIC | 56.0 | 164.8 | 181.4 | 141.7 | 222.0 |

Table (7.7)

Although it should be noted that there is no difference between project based and offshore grid scenario.

### 7.2.5 FRR Activation

The probability distribution of the aggregated reserves deployed during the frequency restoration process in CE and Nordic synchronous areas are depicted in figure 7.15 and 7.16 respectively. As expected, the aggregated FRR in CE reach their limits less than 1% of the times. This is due to the fact that FRR are dimensioned in a way that the FRR capacity of each individual control area equals with the $99^{th}$ percentile of the imbalance occurred in this area.

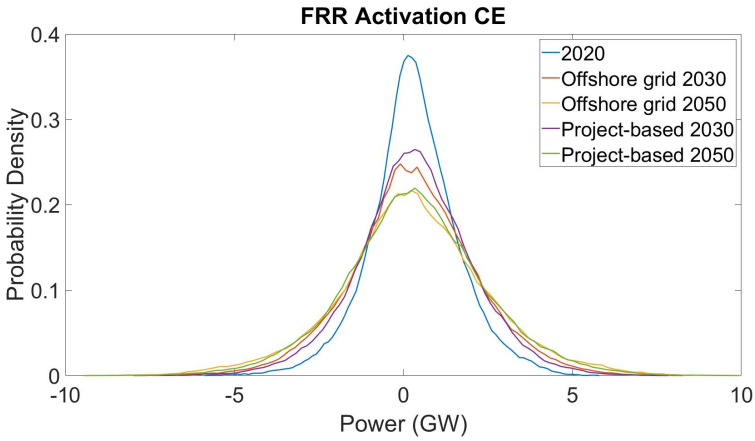


Figure (7.15) Probability distribution function of aggregated FRR deployment in Continental Europe for each scenario and year.

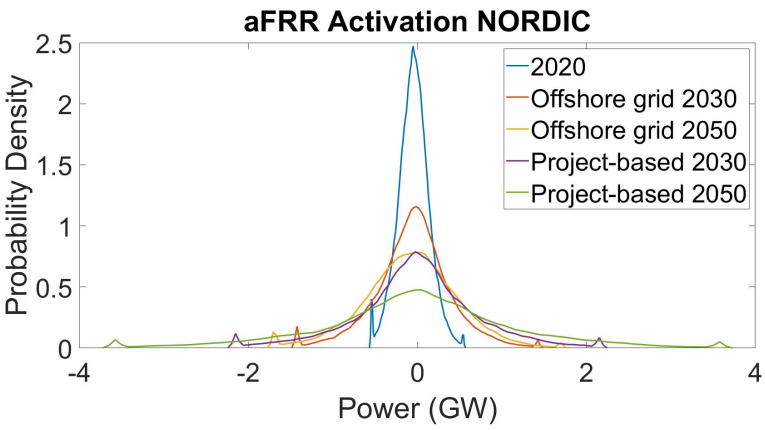


Figure (7.16) Probability distribution function of aggregated aFRR deployment in Nordic synchronous area for each scenario and year.

The probability distribution of the reserves deployed during the frequency restoration process in control area DK1 is illustrated in figure 7.17.

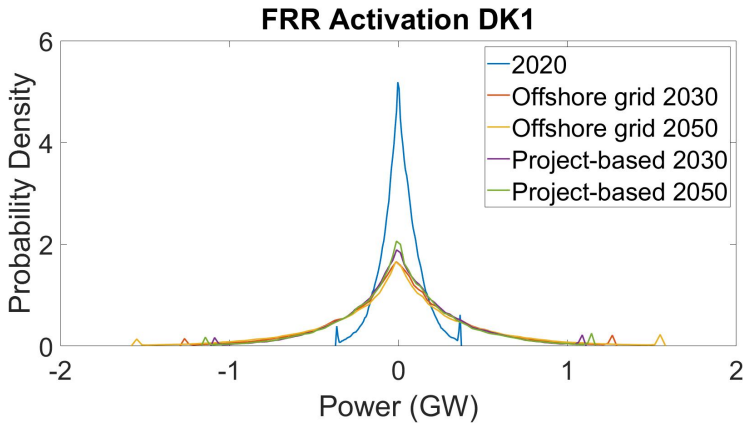


Figure (7.17) Probability distribution function of FRR deployment in DK1 control area for each scenario and year.

The results show that if FRR are properly dimensioned, can be very effective in substantially reducing the requirements for FCR. This is owing to the fact that wind power variability is a slower process as opposed to a disturbance (step change). However, if FRR are not properly dimensioned, wind power forecast error can saturate the FRR activation, resulting in activation of larger volume of FCR.

# Chapter 8

# Conclusion

This report analyses a study in the operation of the power system of Continental Europe and Nordic synchronous areas with focusing on the Danish power system and its regions DK1 and DK2. The study covers all the steps of the operation from the Day Ahead Market til the the Real Time balancing of generation and demand. For that reason, a balancing tool chain has been developed. Furthermore, two scenarios of the future generation and transmission capacity development - Project based and Offshore grid, are considered and simulated for the North Sea countries in 2030 and 2050. The project-based and the offshore grid scenarios represented two different approaches regarding the transmission structure between the North Sea countries of the near future.

The report analyses a) the value of offshore grid on balancing of forecast errors, b) the impact of forecast errors on manual and automatic reserves and c) the quality of electrical frequency in the near future considering high VRE penetration.

The simulation results clearly shows that the offshore grid scenario has very similar impact on balancing of reserves to project based scenario. Since offshore grid scenario provides additional values like increased security and flexibility as well as larger integration of North Sea countries, having similar impact on balancing as that of project based, makes offshore grid an recommendable option for future grid development. Additionally, real-time imbalance in Nordic network is much lower in case of Offshore grid scenario as compared to Project based scenario.

Day ahead market simulations for future shows higher amount of curtailment mainly pertaining to very high volume of installation of wind power. However, the volume of wind power curtailed is still low as compared to the total amount of wind power generation. This being the reason, there is no seasonal pattern in the curtailment of wind power in future scenarios.

Simulations have shown that in future, hour ahead imbalance due to wind forecast error increases in Denmark mainly in DK1. However, the hour ahead imbalance for the whole synchronous area does not increase much. Therefore, intra-hour balancing of Danish control area is largely supported from neighboring regions. Balancing cost which is highly driven by $CO_2$ prices in the simulation, increases substantially towards 2030. Balancing reserves in CE are largely provided by Natural Gas technologies whereas, in Nordic network, bal-

ancing reserves come from Hydro and Natural Gas. Balancing reserves in Denmark mainly come from Natural Gas. However, wind power also increases their role in balancing process in future, mainly in down regulation but also in up regulation especially if wind power is already curtailed in the day-ahead operation.

Real time imbalance seen by Nordic network increases multiple times in 2030 and 2050 scenario as compared to 2020 scenario. Additionally, the real time imbalance in Offshore grid scenario is much lower than that of Project based scenario. Nordic network is also expected to have much lower inertia available in future scenarios as compared to 2020 scenario. The requirement for automatic frequency restoration reserves increases manifold in future scenarios as compared to 2020 scenario. Probabilistic dimensioning of frequency restoration reserves can be beneficial to mitigate the imbalances caused by wind power forecast error mainly in Nordic network. Even with proper dimensioning of frequency restoration reserves, frequency containment reserve for normal operation in Nordic network might be required to be increased in future 2030 and 2050 scenario with very high share of renewables in the power system.

# Bibliography


[1] J. Gea-Bermúdez, K. Das, L.-L. Pade, M. Koivisto, and P. Kanellas. (2019). NSON-DK day-ahead market operation analysis in the north sea region towards 2050 , Technical University of Denmark, [Online]. Available: `https://backend.orbit.dtu.dk/ws/files/202747832/NSON_DK_WP3_D3.1.pdf`.

[2] M. Koivisto and J. Gea-Bermúdez. (2018). NSON-DK energy system scenarios – edition 2, DTU Wind Energy, [Online]. Available: `http://orbit.dtu.dk/files/160234729/NSON_DK_WP2_D2.1.Ed2_FINAL.pdf`.

[3] K. Das, M. J. Koivisto, P. E. Sørensen, and J. Gea-Bermúdez, "Balancing challenges for future north sea offshore network," in *17th International Workshop on Large-Scale Integration of Wind Power into Power Systems as well as on Transmission Networks for Offshore Wind Power Plants*, Energynautics GmbH, 2018.

[4] M. Koivisto, K. Das, F. Guo, P. Sørensen, E. Nuño, N. Cutululis, and P. Maule. (2018). Using time series simulation tool for assessing the effects of variable renewable energy generation on power and energy systems, WIREs Energy and Environment. https://doi.org/10.1002/wene.329.

[5] F. Wiese, R. Bramstoft, H. Koduvere, A. Pizarro Alonso, O. Balyk, J.G. Kirkerud, and H. Ravn. (2018). Balmorel open source energy system model, Energy Strategy Reviews, 20, 26-34. https://doi.org/10.1016/j.esr.2018.01.003.

[6] European Commission, Study of the benefits of a meshed offshore grid in Northern Seas region. (2014), [Online]. Available: `http://ec.europa.eu/energy/en/content/benefits-meshed-offshore-grid-northern-seas-region`.

[7] M. Koivisto et al., *Using time series simulation tool for assessing the effects of variable renewable energy generation on power and energy systems,* Wiley Interdisciplinary Reviews: Energy and Environment, p. e329, 2019.

[8] J. Gea-Bermúdez, K. Das, L.-L. Pade, M. Koivisto, and P. Kanellas, *NSON-DK Day-Ahead market operation analysis in the North Sea region towards 2050*, English. Technical University of Denmark, 2019, ISBN: 978-87-93549-61-6.

[9] P. Kanellas, K. Das, P. E. Sørensen, and J. Gea-Bermudez, "Modelling the intra-hour power system balancing of the danish power system for 2020, 2030 and 2050," in *18th Wind Integration Workshop*, 2019.

[10] K. Das, M. Litong-Palima, P. Maule, and P. E. Sørensen, "Adequacy of operating reserves for power systems in future european wind power scenarios," in *2015 IEEE Power Energy Society General Meeting*, 2015, pages 1–5.

[11] K. Das, M. Litong-Palima, P. Maule, M. Altin, A. D. Hansen, P. E. Sørensen, and H. Abildgaard, "Adequacy of frequency reserves for high wind power generation," *IET Renewable Power Generation*, volume 11, number 8, pages 1286–1294, 2017.

[12] SVENSKA KRAFTNAT, Statnett. (2017). The nordic balancing concept, [Online]. Available: https://www.statnett.no/globalassets/om-statnett/nyheter-og-pressemeldinger/nyhetsarkiv-2018/the-nordic-balancing-concept.pdf.

[13] FINGRID. (2019). Reserves and balancing power, [Online]. Available: https://www.fingrid.fi/en/electricity-market/reserves_and_balancing/#reserve-products.

[14] E. F. Sichani, "Frequency control in future nordic power system with high penetration of wind power," Master's thesis, DTU Wind, Technical University of Denmark, 2017.

[15] Frequency Control in the European Power System Considering the Organisational Structure and Division of Responsibilities. (2016), [Online]. Available: https://doi.org/10.3929/ethz-a-010692129.

[16] Handbook, UCTE Operations. (2009). P1–policy 1: Load-frequency control and performance [c], [Online]. Available: https://www.entsoe.eu/fileadmin/user_upload/_library/publications/entsoe/Operation_Handbook/Policy_1_final.pdf.

[17] ENTSO-E. (2013). Network code on load frequency control and reserves (lfcr), [Online]. Available: https://www.entsoe.eu/major-projects/network-code-development/load-frequency-control-reserves/Pages/default.aspx.

# Appendix A

# Mathematical model formulation of Day Ahead Market Model in Balmorel

## A.1 Methodology

The temporal representation used consists of years $y \in \mathbb{Y}$ , which are disaggregated into seasons $s \in \mathbb{S}$ which are composed of time steps $t \in \mathbb{T}$ . For the simulations of Day Ahead market the season represent days and time steps represent hours. Regarding the geographical representation, there are three gradation: countries consisting of regions $r \in \mathbb{R}$, which are disaggregated into areas $a \in \mathbb{A}$. Regions represent copperplate zones for electricity transmission, whereas areas represent copperplate zones for heat transmission.

The methodology used to simulate the Day-Ahead market can be split in three groups: Storage and planned maintenance optimisation , Stochastic outage simulations and Day-Ahead optimisation. As already mentioned, the optimisations are performed with the energy system model Balmorel and the VRE generation time series where calculated with the simulation tool CorRES.

The Storage and planned maintenance optimisation is run in order to capture the decision that need to be made from the market participants based on future expectations of market prices and not just on the next 24 hours. The maintenance time is technology specific and the generators choose when they will be inoperative considering the losses coming from their absence from the market. In addition, in order to maximize their profit storage units have to load during seasons with low prices and unload in seasons with high prices. These two decisions are made by running the Storage and planned maintenance optimisation model for a full year, saving the results at the beginning of each season and forcing them during the Day Ahead optimization.

In order to introduce the stochasticity of an unexpected operational problem in the model the Stochastic outage simulation is used. The stochastic outages are modelled by considering the total capacity of a unit type in each area, the size of a single unit, the planned maintenance, and the probability of suffering an outage. The outages are assumed to last 1 hour and Monte Carlo simulations are performed for every time step and unit.

The results of these simulation are also forced during the Day Ahead market optimization.

## A.2 Mathematical model formulation

### A.2.1 Day-Ahead optimisation formulation

#### Objective function

The objective function is to minimize the operational costs of the studied system for each time step. In Day Ahead market the time steps considered in this optimisation correspond to one hour. Its year is optimized separately as the years are not linked. In this report, these costs have been aggregated into to fixed operational and maintenance costs (fom), variable operational and maintenance costs (vom), unit commitment related costs (uc), emission tax costs (emi), and transmission use costs (trans).

$$\min \sum_{y \in \mathbb{Y}} c_y^{fom} + c_y^{vom} + c_y^{uc} + c_y^{emi} + c_y^{trans} \tag{A.1}$$

**Fixed O&M costs**

Fixed costs depict the annual availability cost to be paid regardless of the use of each technology:

$$\begin{aligned} c_y^{fom} = \sum_{a \in \mathbb{A}} \Bigg( & \sum_{g \in \mathbb{E}} FC_{g,a,y} \cdot \eta^{el} \cdot C_g^{fom} \\ & + \sum_{g \in \mathbb{H}, g \notin \mathbb{CHP}} FC_{g,a,y} \cdot \eta^{h} \cdot C_g^{fom} \Bigg) \\ & \forall y \in \mathbb{Y} \end{aligned} \tag{A.2}$$

**Variable Operational and Maintenance costs**

Variable operation and maintenance costs depict fuel (f) consumption costs, as well as the cost related with normal operation (oper) (e.g. consumption of auxiliary materials, maintenance, etc):

$$\begin{aligned} c_y^{vom} = \sum_{a \in \mathbb{A}} \sum_{s \in \mathbb{S}} \sum_{t \in \mathbb{T}} \Bigg( & \sum_{g \in \mathbb{G}, g \notin \mathbb{PTOH}} d_{g,a,y,s,t}^{f} \cdot C_{g,a,y}^{f} \\ & + \sum_{g \in \mathbb{EL}, g \notin \mathbb{CHP}} p_{g,a,y,s,t}^{el} \cdot C_g^{oper} \\ & + \sum_{g \in \mathbb{H}, g \notin \mathbb{CHP}} p_{g,a,y,s,t}^{h} \cdot C_g^{oper} \\ & + \sum_{g \in \mathbb{CHP}} d_{g,a,y,s,t}^{f} \cdot C_g^{oper} \Bigg) \\ & \forall y \in \mathbb{Y} \end{aligned} \tag{A.3}$$

**Unit Commitment costs**

Unit commitment costs depict the expenses caused from starting up (su), shuting down (sd) and online costs (on):

$$
\begin{aligned}
c_y^{uc} = \sum_{a\in\mathbb{A}}\sum_{s\in\mathbb{S}}\sum_{t\in\mathbb{T}}\Bigg(&\sum_{g\in\mathbb{G}} n_{g,a,y,s,t}^{av,su}\cdot US_g^{gen}\cdot C_g^{su} \\
&+\sum_{g\in\mathbb{G}} n_{g,a,y,s,t}^{av,sd}\cdot US_g^{gen}\cdot C_g^{sd} \\
&+\sum_{g\in\mathbb{G}} n_{g,a,y,s,t}^{av,on}\cdot US_g^{gen}\cdot C_g^{on} \\
&+\sum_{g\in\mathbb{STO}} (n_{g,a,y,s,t}^{av,su}\cdot \frac{US_{g,a,y}^{sto}}{HU_g^{sto}} \\
&+ston_{g,a,y,s,t}^{av,su}\cdot \frac{US_{g,a,y}^{sto}}{HL_g^{sto}})\cdot C_g^{su} \\
&+\sum_{g\in\mathbb{STO}} (n_{g,a,y,s,t}^{av,sd}\cdot \frac{US_{g,a,y}^{sto}}{HU_g^{sto}} \\
&+ston_{g,a,y,s,t}^{av,sd}\cdot \frac{US_{g,a,y}^{sto}}{HL_g^{sto}})\cdot C_g^{sd} \\
&+\sum_{g\in\mathbb{STO}} (n_{g,a,y,s,t}^{av,on}\cdot \frac{US_{g,a,y}^{sto}}{HU_g^{sto}} \\
&+ston_{g,a,y,s,t}^{av,on}\cdot \frac{US_{g,a,y}^{sto}}{HL_g^{sto}})\cdot C_g^{on}\Bigg) \\
&\forall y\in\mathbb{Y}
\end{aligned}
\tag{A.4}
$$

**Emission costs**

Emissions (emi) costs represent the tax-related expense incurred by those generation technologies emitting $CO_2$:

$$
c_y^{emi} = \sum_{a\in\mathbb{A}}\sum_{s\in\mathbb{S}}\sum_{t\in\mathbb{T}}\sum_{g\in\mathbb{G},g\notin\mathbb{PTOH}} d_{g,a,y,s,t}^{f}\cdot C_{g,y}^{CO_2} \qquad \forall y\in\mathbb{Y} \tag{A.5}
$$

**Trans costs**

Transmission (trans) costs account for the expense of transmission lines utilization:

$$
c_y^{trans} = \sum_{s\in\mathbb{S}}\sum_{t\in\mathbb{T}}\sum_{r\in\mathbb{R}}\sum_{r'\in\mathbb{R}}\Big(x_{r,r',y,s,t}\cdot C^{trans}) \qquad \forall y\in\mathbb{Y} \tag{A.6}
$$

**System constraints**

The systems constraints included are the electricity balance, heat balance, and ancillary services in the electricity market.

**Electricity Balance**

In the electricity balance the use of the electricity storage is optimized and most of the electricity demand is considered inelastic, except for the use of power to heat in district heating networks.

$$\begin{aligned}\sum_{a\in\mathbb{AR}}\Bigg(\sum_{g\in\mathbb{EL}} p^{el}_{g,a,y,s,t} - \sum_{g\in\mathbb{STO},g\in\mathbb{EL}} stol_{g,a,y,s,t} \\ - \sum_{g\in\mathbb{PTOH}} d^{f}_{g,a,y,s,t}\Bigg) = D^{el}_{r,y,s,t} \\ + \sum_{r'\in\mathbb{R}}\Big(x_{r,r',y,s,t} - x_{r',r,y,s,t}\cdot(1-xloss)\Big) \\ \forall r\in\mathbb{R}, y\in\mathbb{Y}, s\in\mathbb{S}, t\in\mathbb{T}\end{aligned} \tag{A.7}$$

**Heat Balance**

In the heat balance constrain the utilization of heat storage is optimized and the heat demand considered inelastic.

$$\begin{aligned}\sum_{g\in\mathbb{HEAT}} p^{h}_{g,a,y,s,t} - \sum_{g\in\mathbb{STO},g\in\mathbb{H}} stol_{g,a,y,s,t} = D^{h}_{a,y,s,t} \\ \forall a\in\mathbb{A}, y\in\mathbb{Y}, s\in\mathbb{S}, t\in\mathbb{T}\end{aligned} \tag{A.8}$$

**Ancillary Services**

The constrains of this subsection ensure that the required amount of automatic reserves will be kept in the DA dispatch schedule and will be available for deployment in the last part of the tool chain ( chapter: 2), the Area Control Dynamic Model. The allocation of reserves could change in the balopt optimization though. It is worth it to mention that the constrains regarding mFRR and mRR are not included in the current optimization runs.

**FCR**

$$\begin{aligned}\sum_{a\in\mathbb{AR}}\sum_{g\in\mathbb{FCRU}} fcr^{up}_{g,a,y,s,t} \geq FCR^{up}_{y,r} \\ \forall y\in\mathbb{Y}, s\in\mathbb{S}, t\in\mathbb{T}\end{aligned} \tag{A.9}$$

$$\begin{aligned}\sum_{a\in\mathbb{AR}}\sum_{g\in\mathbb{FCRD}} fcr^{dn}_{g,a,y,s,t} \geq FCR^{dn}_{y,r} \\ \forall y\in\mathbb{Y}, s\in\mathbb{S}, t\in\mathbb{T}\end{aligned} \tag{A.10}$$

$$\sum_{r\in\mathbb{RC}}\sum_{a\in\mathbb{AR}}\sum_{g\in\mathbb{FCRU}} fcr^{up}_{g,a,y,s,t} \geq FCR^{up}_{y,c} \quad \forall y \in \mathbb{Y}, s \in \mathbb{S}, t \in \mathbb{T} \tag{A.11}$$

$$\sum_{r\in\mathbb{RC}}\sum_{a\in\mathbb{AR}}\sum_{g\in\mathbb{FCRD}} fcr^{dn}_{g,a,y,s,t} \geq FCR^{dn}_{y,c} \quad \forall y \in \mathbb{Y}, s \in \mathbb{S}, t \in \mathbb{T} \tag{A.12}$$

**<u>aFRR</u>**

$$\sum_{a\in\mathbb{AR}}\sum_{g\in\mathbb{AFRU}} afrr^{up}_{g,a,y,s,t} \geq AFR^{up}_{y,r} \quad \forall y \in \mathbb{Y}, s \in \mathbb{S}, t \in \mathbb{T} \tag{A.13}$$

$$\sum_{a\in\mathbb{AR}}\sum_{g\in\mathbb{AFRD}} afrr^{dn}_{g,a,y,s,t} \geq AFR^{dn}_{y,r} \quad \forall y \in \mathbb{Y}, s \in \mathbb{S}, t \in \mathbb{T} \tag{A.14}$$

$$\sum_{r\in\mathbb{RC}}\sum_{a\in\mathbb{AR}}\sum_{g\in\mathbb{AFRU}} afrr^{up}_{g,a,y,s,t} \geq AFR^{up}_{y,c} \quad \forall y \in \mathbb{Y}, s \in \mathbb{S}, t \in \mathbb{T} \tag{A.15}$$

$$\sum_{r\in\mathbb{RC}}\sum_{a\in\mathbb{AR}}\sum_{g\in\mathbb{AFRD}} afrr^{dn}_{g,a,y,s,t} \geq AFR^{dn}_{y,c} \quad \forall y \in \mathbb{Y}, s \in \mathbb{S}, t \in \mathbb{T} \tag{A.16}$$

**<u>mFRR</u>**

$$\sum_{a\in\mathbb{AR}}\sum_{g\in\mathbb{MFRU}} mfrr^{up}_{g,a,y,s,t} \geq MFR^{up}_{y,r} \quad \forall y \in \mathbb{Y}, s \in \mathbb{S}, t \in \mathbb{T} \tag{A.17}$$

$$\sum_{a\in\mathbb{AR}}\sum_{g\in\mathbb{MFRD}} mfrr^{dn}_{g,a,y,s,t} \geq MFR^{dn}_{y,r} \quad \forall y \in \mathbb{Y}, s \in \mathbb{S}, t \in \mathbb{T} \tag{A.18}$$

$$\sum_{r\in\mathbb{RC}}\sum_{a\in\mathbb{AR}}\sum_{g\in\mathbb{MFRU}} mfrr^{up}_{g,a,y,s,t} \geq MFR^{up}_{y,c} \quad \forall y \in \mathbb{Y}, s \in \mathbb{S}, t \in \mathbb{T} \tag{A.19}$$

$$\sum_{r\in\mathbb{RC}}\sum_{a\in\mathbb{AR}}\sum_{g\in\mathbb{MFRD}} mfrr^{dn}_{g,a,y,s,t} \geq MFR^{dn}_{y,c} \quad \forall y\in\mathbb{Y}, s\in\mathbb{S}, t\in\mathbb{T} \tag{A.20}$$

**<u>mRR</u>**

$$\sum_{a\in\mathbb{AR}}\sum_{g\in\mathbb{MRRU}} mrr^{up}_{g,a,y,s,t} \geq MRR^{up}_{y,r} \quad \forall y\in\mathbb{Y}, s\in\mathbb{S}, t\in\mathbb{T} \tag{A.21}$$

$$\sum_{a\in\mathbb{AR}}\sum_{g\in\mathbb{MRRD}} mrr^{dn}_{g,a,y,s,t} \geq MRR^{dn}_{y,r} \quad \forall y\in\mathbb{Y}, s\in\mathbb{S}, t\in\mathbb{T} \tag{A.22}$$

$$\sum_{r\in\mathbb{RC}}\sum_{a\in\mathbb{AR}}\sum_{g\in\mathbb{MRRU}} mrr^{up}_{g,a,y,s,t} \geq MRR^{up}_{y,c} \quad \forall y\in\mathbb{Y}, s\in\mathbb{S}, t\in\mathbb{T} \tag{A.23}$$

$$\sum_{r\in\mathbb{RC}}\sum_{a\in\mathbb{AR}}\sum_{g\in\mathbb{MRRD}} mrr^{dn}_{g,a,y,s,t} \geq MRR^{dn}_{y,c} \quad \forall y\in\mathbb{Y}, s\in\mathbb{S}, t\in\mathbb{T} \tag{A.24}$$

**<u>Ancillary Service Capacity Limits from pure storage units</u>**

Only pure storage units already online from the DA are allowed to participate in IH. The maximum capacity of storage units kept for automatic resrve's up is defined in equation A.25.

$$\begin{aligned} fcr^{up}_{g,a,y,s,t} + afrr^{up}_{g,a,y,s,t} \leq \frac{US^{sto}_g}{HU_g}\cdot n^{on}_{g,a,y,s,t} - p^{el}_{g,a,y,s,t} + \\ stol_{g,a,y,s,t} - \frac{US^{sto}_g}{HL_g}\cdot ston^{on}_{g,a,y,s,t}\cdot MO_g \\ \forall g\in\mathbb{STO}, a\in\mathbb{A}, y\in\mathbb{Y}, s\in\mathbb{S}, t\in\mathbb{T} \end{aligned} \tag{A.25}$$

The maximum capacity of storage units kept for automatic resrve's down is defined in equation A.28.

$$\begin{aligned} fcr^{dn}_{g,a,y,s,t} + afrr^{dn}_{g,a,y,s,t} \leq ston^{on}_{g,a,y,s,t}\cdot\frac{US^{sto}_g}{HL_g} - stol_{g,a,y,s,t} + \\ p^{el}_{g,a,y,s,t} - n^{on}_{g,a,y,s,t} cdot \frac{US^{sto}_g}{HU_g}\cdot MO_g \\ \forall g\in\mathbb{STO}, a\in\mathbb{A}, y\in\mathbb{Y}, s\in\mathbb{S}, t\in\mathbb{T} \end{aligned} \tag{A.26}$$

**Ancillary Service Energy Limits from pure storage units**

$$soc_{g,a,y,s,t} + TL_{s,t} \cdot (stol_{g,a,y,s,t} - \frac{p^{el}_{g,a,y,s,t}}{\eta^{sto}_g}) \geq \frac{fcr^{up}_{g,a,y,s,t} + afrr^{up}_{g,a,y,s,t}}{\eta^{sto}_g} \tag{A.27}$$

$$\frac{FC_{g,a,y}}{\eta^{sto}_g} - soc_{g,a,y,s,t} + TL_{s,t} \cdot \left(stol_{g,a,y,s,t} - \frac{p^{el}_{g,a,y,s,t}}{\eta^{sto}_g}\right) \geq fcr^{dn}_{g,a,y,s,t} + afrr^{dn}_{g,a,y,s,t} \tag{A.28}$$

**Technological constraints for dispatchable generation units**

Dispatchable technologies include power-only, CHP, boilers, heat pumps, geothermal, and hydroelectric power with reservoirs. These units are subject to several technical constraints.

**Available units**

The maximum number of available units for generation depends on the installed capacity, unit size, and Availability Factor (AF):

$$\frac{FC_{g,a,y}}{US^{gen}_g} \cdot AF_{g,a,y,s,t} \geq n^{av,on}_{g,a,y,s,t} \quad \forall g \in \mathbb{GD}, a \in \mathbb{A}, y \in \mathbb{Y}, s \in \mathbb{S}, t \in \mathbb{T} \tag{A.29}$$

The parameter AF depends on installed capacity, unit size, units under planned maintenance and units under forced outage:

$$AF_{g,a,y,s,t} = max\left\{1 - \frac{US^{gen}_g \cdot (n^{nav,pm}_{g,a,y,s} + n^{nav,so}_{g,a,y,s,t})}{FC_{g,a,y}}, 0\right\} \quad \forall g \in \mathbb{GD}, a \in \mathbb{A}, y \in \mathbb{Y}, s \in \mathbb{S}, t \in \mathbb{T} \tag{A.30}$$

The number of units on planned maintenance is taken from the storage and planned maintenance optimization. The number of units under forced outage is taken from the stochastic outage simulations.

**Fuel consumption limits**

The consumption of fuel from the generators is modeled through the constrains presented in this subsection. The maximum and minimum fuel consumption constrains are presented in equations A.31 and A.32 respectively.

$$US^{gen}_g \cdot n^{av,on}_{g,a,y,s,t} \geq d^f_{g,a,y,s,t} \quad \forall g \in \mathbb{GD}, a \in \mathbb{A}, y \in \mathbb{Y}, s \in \mathbb{S}, t \in \mathbb{T} \tag{A.31}$$

$$d^{f}_{g,a,y,s,t} \geq US^{gen}_{g} \cdot n^{av,on}_{g,a,y,s,t} \cdot MO_{g}$$
$$\forall g \in \mathbb{GD}, a \in \mathbb{A}, y \in \mathbb{Y}, s \in \mathbb{S}, t \in \mathbb{T} \tag{A.32}$$

**Ramping constraints**

The constrains representing the ramping of generators are presented bellow. Ramping up and ramping down is simulated based on the equations A.33 and A.34 respectively.

$$d^{f}_{g,a,y,s,t} - d^{f}_{g,a,y,s,t-1} \leq$$
$$US^{gen}_{g} \cdot (n^{av,on}_{g,a,y,s,t} - n^{av,su}_{g,a,y,s,t}) \cdot RR^{up}_{g} \tag{A.33}$$
$$\forall g \in \mathbb{PO}, a \in \mathbb{A}, y \in \mathbb{Y}, s \in \mathbb{S}, t \in \mathbb{T}$$

$$d^{f}_{g,a,y,s,t-1} - d^{f}_{g,a,y,s,t} \leq$$
$$US^{gen}_{g} \cdot (n^{av,on}_{g,a,y,s,t} + n^{av,sd}_{g,a,y,s,t}) \cdot RR^{down}_{g} \tag{A.34}$$
$$\forall g \in \mathbb{PO}, a \in \mathbb{A}, y \in \mathbb{Y}, s \in \mathbb{S}, t \in \mathbb{T}$$

**Minimum on/off time constraints**

Some of the generators have to be on or off for at least a pre-defined minimum time before their state is changed. The minimum on and off time constrains are presented in equations A.35 and A.36 respectively.

$$\sum_{t'=1}^{MUT_g} n^{av,su}_{g,a,y,s,t-t'} \leq n^{av,on}_{g,a,y,s,t} \tag{A.35}$$
$$\forall g \in \mathbb{PO}, a \in \mathbb{A}, y \in \mathbb{Y}, s \in \mathbb{S}, t \in \mathbb{T}$$

$$\sum_{t'=1}^{MDT_g} n^{av,sd}_{g,a,y,s,t-t'} \leq \frac{FC_{g,a,y}}{US^{gen}_{g}} - n^{av,on}_{g,a,y,s,t} \tag{A.36}$$
$$\forall g \in \mathbb{PO}, a \in \mathbb{A}, y \in \mathbb{Y}, s \in \mathbb{S}, t \in \mathbb{T}$$

**Logical conditions**

$$n^{av,on}_{g,a,y,s,t} - n^{av,on}_{g,a,y,s,t-1} = n^{av,su}_{g,a,y,s,t} - n^{av,sd}_{g,a,y,s,t} \tag{A.37}$$
$$\forall g \in \mathbb{GD}, a \in \mathbb{A}, y \in \mathbb{Y}, s \in \mathbb{S}, t \in \mathbb{T}$$

In order to reflect the discrete nature of the generation units that are part of the energy system, the following variables are restricted to be integer variables. In case that reducing the computational time is essential, this constrain can be relaxed and it's variables become continuous.

$$n^{av,on}_{g,a,y,s,t}, n^{av,su}_{g,a,y,s,t}, n^{av,sd}_{g,a,y,s,t} \in \mathbb{Z}^+ \\ \forall g \in \mathbb{GD}, a \in \mathbb{A}, y \in \mathbb{Y}, s \in \mathbb{S}, t \in \mathbb{T} \tag{A.38}$$

**Specific technological constraints for power only thermal plants**

The installed capacity represents the maximum net generation of power. Technologies involved are gas and steam turbines, engines, and combined cycles.

$$d^f_{g,a,y,s,t} \cdot \eta^{el}_g \geq p^{el}_{g,a,y,s,t} \\ \forall g \in \mathbb{PO}, a \in \mathbb{A}, y \in \mathbb{Y}, s \in \mathbb{S}, t \in \mathbb{T} \tag{A.39}$$

**Specific technological constraints for heat only producers**

The installed capacity represents the maximum net generation of heat. Technologies involved are fuel boilers and Power-to-Heat units.

$$d^f_{g,a,y,s,t} \cdot \eta^h_g = p^h_{g,a,y,s,t} \\ \forall g \in \mathbb{HO}, a \in \mathbb{A}, y \in \mathbb{Y}, s \in \mathbb{S}, t \in \mathbb{T} \tag{A.40}$$

**Specific technological constraints for Combined Heat and Power thermal plants**

Back pressure technologies present linear relation between electricity and heat generation (CB line).

$$p^e_{g,a,y,s,t} = p^h_{g,a,y,s,t} \cdot CB_g \\ \forall g \in \mathbb{BP}, a \in \mathbb{A}, y \in \mathbb{Y}, s \in \mathbb{S}, t \in \mathbb{T} \tag{A.41}$$

Their fuel demand depends on the electrical efficiency and production:

$$d^f_{g,a,y,s,t} \cdot \eta^{el}_g = p^e_{g,a,y,s,t} \\ \forall g \in \mathbb{BP}, a \in \mathbb{A}, y \in \mathbb{Y}, s \in \mathbb{S}, t \in \mathbb{T} \tag{A.42}$$

On the other hand, extraction power plans have a more flexible range of operation of heat and power. They are capable of producing power without producing heat, but not otherwise. The CB and CV (iso-fuel) parameter define the operational range:

$$p^e_{g,a,y,s,t} \geq p^h_{g,a,y,s,t} \cdot CB_g \\ \forall g \in \mathbb{EXT}, a \in \mathbb{A}, y \in \mathbb{Y}, s \in \mathbb{S}, t \in \mathbb{T} \tag{A.43}$$

$$US^{gen}_g \cdot n^{on}_{g,a,y,s,t} \cdot \eta^{el}_g \geq p^e_{g,a,y,s,t} + p^h_{g,a,y,s,t} \cdot CV_g \\ \forall g \in \mathbb{EXT}, a \in \mathbb{A}, y \in \mathbb{Y}, s \in \mathbb{S}, t \in \mathbb{T} \tag{A.44}$$

$$d^{f}_{g,a,y,s,t} \cdot \eta^{el}_{g} = p^{e}_{g,a,y,s,t} + p^{h}_{g,a,y,s,t} \cdot CV_{g} \quad \forall g \in \mathbb{BP}, a \in \mathbb{A}, y \in \mathbb{Y}, s \in \mathbb{S}, t \in \mathbb{T} \tag{A.45}$$

**Specific technological constraints for hydro power plants with seasonal inflow**

Hydroelectric power with reservoirs are modelled as a generation technology linked to storage with limited energy capacity and that receives seasonal energy inflows. The model optimizes the production and level of storage along the year, with the condition that the level of the storage at the beginning of the simulated year equals the level at the end. The level at the beginning of each season is forced from the storage and planned maintenance optimisation.

$$hsl_{a,y,s+1} \geq hsl_{a,y,s} + HI_{a,s} + \sum_{t \in \mathbb{T}} \sum_{g \in \mathbb{HYD}} TL_{s,t} \cdot \frac{p^{el}_{g,a,y,s,t}}{\eta^{el}_{g}} \quad \forall a \in \mathbb{A}, y \in \mathbb{Y}, s \in \mathbb{S} \tag{A.46}$$

$$\overline{HSL}_{a,s} \geq hsl_{a,y,s} \quad \forall a \in \mathbb{A}, y \in \mathbb{Y}, s \in \mathbb{S} \tag{A.47}$$

$$\underline{HSL}_{a,s} \leq hsl_{a,y,s} \quad \forall a \in \mathbb{A}, y \in \mathbb{Y}, s \in \mathbb{S} \tag{A.48}$$

**Technological constraints for pure storage units**

Those storage units that do not receive inflow except from the active loading are defined as pure storage units. Examples of these technologies are hydro pumping, power batteries, and hot water tanks, or pit heat storage.
The main equation for pure storage is the storage balance, which for these technologies is calculated for every t. The level at the beginning of each season is forced from the storage and planned maintenance optimisation. Fuel demand equals in this case electricity, or heat, production:

**Storage balance**

The equation B.4 simulates the state of charge of pure storage technologies.

$$soc_{g,a,y,s,t+1} = soc_{g,a,y,s,t} + TL_{s,t} \cdot (stol_{g,a,y,s,t} - \frac{p^{f}_{g,a,y,s,t}}{\eta^{sto}_{g}}) \quad \forall g \in \mathbb{STO}, a \in \mathbb{A}, y \in \mathbb{Y}, s \in \mathbb{S}, t \in \mathbb{T} \tag{A.49}$$

**Available units**

The equations A.50 and A.51 model the maximum number of units available for unloading and loading for pure storage technologies respectively.

$$\frac{EC_{g,a,y}}{US_g^{sto}} \cdot AF_{g,a,y,s,t} \geq n_{g,a,y,s,t}^{av,on} \quad \forall g \in \mathbb{STO}, a \in \mathbb{A}, y \in \mathbb{Y}, s \in \mathbb{S}, t \in \mathbb{T} \tag{A.50}$$

$$\frac{EC_{g,a,y}}{US_g^{sto}} \cdot AF_{g,a,y,s,t} \geq ston_{g,a,y,s,t}^{av,on} \quad \forall g \in \mathbb{STO}, a \in \mathbb{A}, y \in \mathbb{Y}, s \in \mathbb{S}, t \in \mathbb{T} \tag{A.51}$$

The availability factor is constraint by the storage itself, so the assumption is that if the storage is not available, it is not available for loading nor unloading.

$$AF_{g,a,y,s,t} = max\left\{1 - \frac{US_g \cdot (n_{g,a,y,s}^{nav,pm} + n_{g,a,y,s,t}^{nav,so})}{K_g^G}, 0\right\} \quad \forall g \in \mathbb{STO}, a \in \mathbb{A}, y \in \mathbb{Y}, s \in \mathbb{S}, t \in \mathbb{T} \tag{A.52}$$

**Storage loading and unloading limits**

The maximum allowed unloading of pure storage units is defined in equations A.53 and A.54.

$$\frac{US_g^{sto}}{HU_g} \cdot n_{g,a,y,s,t}^{av,on} \geq p_{g,a,y,s,t}^{el} \quad \forall g \in \mathbb{STOEL}, a \in \mathbb{A}, y \in \mathbb{Y}, s \in \mathbb{S}, t \in \mathbb{T} \tag{A.53}$$

$$\frac{US_g^{sto}}{HU_g} \cdot n_{g,a,y,s,t}^{av,on} \geq p_{g,a,y,s,t}^{h} \quad \forall g \in \mathbb{STOH}, a \in \mathbb{A}, y \in \mathbb{Y}, s \in \mathbb{S}, t \in \mathbb{T} \tag{A.54}$$

The maximum allowed loading of pure storage units is defined in equation A.55.

$$\frac{US_g^{sto}}{HL_g} \cdot ston_{g,a,y,s,t}^{on} \geq stol_{g,a,y,s,t} \quad \forall g \in \mathbb{STO}, a \in \mathbb{A}, y \in \mathbb{Y}, s \in \mathbb{S}, t \in \mathbb{T} \tag{A.55}$$

The minimum allowed unloading of pure storage units is defined in equations A.56 and A.57.

$$\frac{US_g^{sto}}{HU_g} \cdot n_{g,a,y,s,t}^{on} \cdot MO_g \cdot \leq p_{g,a,y,s,t}^{el} \quad \forall g \in \mathbb{STOEL}, a \in \mathbb{A}, y \in \mathbb{Y}, s \in \mathbb{S}, t \in \mathbb{T} \tag{A.56}$$

$$\frac{US_g^{sto}}{HU_g} \cdot n_{g,a,y,s,t}^{on} \cdot MO_g \leq p_{g,a,y,s,t}^{h} \tag{A.57}$$
$$\forall g \in \mathbb{STOH}, a \in \mathbb{A}, y \in \mathbb{Y}, s \in \mathbb{S}, t \in \mathbb{T}$$

The minimum allowed loading of pure storage units is defined in equation A.58.

$$\frac{US_g^{sto}}{HL_g} \cdot ston_{g,a,y,s,t}^{on} \cdot MO_g \geq stol_{g,a,y,s,t} \tag{A.58}$$
$$\forall g \in \mathbb{STO}, a \in \mathbb{A}, y \in \mathbb{Y}, s \in \mathbb{S}, t \in \mathbb{T}$$

**Ramping constraints**

The constrains modeling the ramping up of pure storage units during unloading presented in equations A.59 and A.60.

$$p_{g,a,y,s,t}^{el} - p_{g,a,y,s,t-1}^{el} \leq$$
$$\frac{US_g^{sto}}{HU_g} \cdot (n_{g,a,y,s,t}^{av,on} - n_{g,a,y,s,t}^{av,su}) \cdot RR_g^{up} \tag{A.59}$$
$$\forall g \in \mathbb{STO}, g \in \mathbb{EL}, a \in \mathbb{A}, y \in \mathbb{Y}, s \in \mathbb{S}, t \in \mathbb{T}$$

$$p_{g,a,y,s,t}^{h} - p_{g,a,y,s,t-1}^{h} \leq$$
$$\frac{US_g^{sto}}{HU_g} \cdot (n_{g,a,y,s,t}^{av,on} - n_{g,a,y,s,t}^{av,su}) \cdot RR_g^{up} \tag{A.60}$$
$$\forall g \in \mathbb{STO}, g \in \mathbb{HEAT}, a \in \mathbb{A}, y \in \mathbb{Y}, s \in \mathbb{S}, t \in \mathbb{T}$$

The ramping up of pure storage units during loading is modeled through equation A.61.

$$stol_{g,a,y,s,t} - stol_{g,a,y,s,t-1} \leq$$
$$\frac{US_g^{sto}}{HL_g} \cdot (n_{g,a,y,s,t}^{av,on} - n_{g,a,y,s,t}^{av,su}) \cdot RR_g^{up} \tag{A.61}$$
$$\forall g \in \mathbb{STO}, a \in \mathbb{A}, y \in \mathbb{Y}, s \in \mathbb{S}, t \in \mathbb{T}$$

Similarly, the modeling of ramping down in case of unloading is done from the constrains A.59 and A.60.

$$p_{g,a,y,s,t-1}^{el} - p_{g,a,y,s,t}^{el} \leq$$
$$\frac{US_g^{sto}}{HU_g} \cdot (n_{g,a,y,s,t}^{av,on} - n_{g,a,y,s,t}^{av,su}) \cdot RR_g^{down} \tag{A.62}$$
$$\forall g \in \mathbb{STO}, g \in \mathbb{EL}, a \in \mathbb{A}, y \in \mathbb{Y}, s \in \mathbb{S}, t \in \mathbb{T}$$

$$p^{h}_{g,a,y,s,t-1} - p^{h}_{g,a,y,s,t} \leq \frac{US^{sto}_{g}}{HU_{g}} \cdot (n^{av,on}_{g,a,y,s,t} - n^{av,su}_{g,a,y,s,t}) \cdot RR^{down}_{g} \quad \forall g \in \mathbb{STO}, g \in \mathbb{HEAT}, a \in \mathbb{A}, y \in \mathbb{Y}, s \in \mathbb{S}, t \in \mathbb{T} \tag{A.63}$$

The ramping down of pure storage units during loading is simulated through the equation A.64.

$$stol_{g,a,y,s,t-1} - stol_{g,a,y,s,t} \leq \frac{US^{sto}_{g}}{HL_{g}} \cdot (n^{av,on}_{g,a,y,s,t} - n^{av,su}_{g,a,y,s,t}) \cdot RR^{down}_{g} \quad \forall g \in \mathbb{STO}, a \in \mathbb{A}, y \in \mathbb{Y}, s \in \mathbb{S}, t \in \mathbb{T} \tag{A.64}$$

**Minimum on/off time constraints**

The minimum on time during unloading and loading is defined through the equations A.65 and A.66 respectively.

$$\sum_{t'=1}^{MUT_g} n^{av,su}_{g,a,y,s,t-t'} \leq n^{av,on}_{g,a,y,s,t} \quad \forall g \in \mathbb{STO}, a \in \mathbb{A}, y \in \mathbb{Y}, s \in \mathbb{S}, t \in \mathbb{T} \tag{A.65}$$

$$\sum_{t'=1}^{MUT_g} ston^{av,su}_{g,a,y,s,t-t'} \leq ston^{av,on}_{g,a,y,s,t} \quad \forall g \in \mathbb{STO}, a \in \mathbb{A}, y \in \mathbb{Y}, s \in \mathbb{S}, t \in \mathbb{T} \tag{A.66}$$

The minimum off time during unloading and loading is defined through the equations A.67 and A.68 respectively.

$$\sum_{t'=1}^{MDT_g} n^{av,sd}_{g,a,y,s,t-t'} \leq \frac{EC_{g,a,y}}{US^{sto}_{g}} - n^{av,on}_{g,a,y,s,t} \quad \forall g \in \mathbb{STO}, a \in \mathbb{A}, y \in \mathbb{Y}, s \in \mathbb{S}, t \in \mathbb{T} \tag{A.67}$$

$$\sum_{t'=1}^{MDT_g} ston^{av,sd}_{g,a,y,s,t-t'} \leq \frac{EC_{g,a,y}}{US^{sto}_{g}} - ston^{av,on}_{g,a,y,s,t} \quad \forall g \in \mathbb{STO}, a \in \mathbb{A}, y \in \mathbb{Y}, s \in \mathbb{S}, t \in \mathbb{T} \tag{A.68}$$

**Logical conditions**

Logical conditions regarding the unloadin and loading procedure of pure storage units are presented in equations A.69 and A.70 respectively.

$$n^{av,on}_{g,a,y,s,t} - n^{av,on}_{g,a,y,s,t-1} = n^{av,su}_{g,a,y,s,t} - n^{av,sd}_{g,a,y,s,t} \\ \forall g \in \mathbb{STO}, a \in \mathbb{A}, y \in \mathbb{Y}, s \in \mathbb{S}, t \in \mathbb{T} \tag{A.69}$$

$$ston^{av,on}_{g,a,y,s,t} - ston^{av,on}_{g,a,y,s,t-1} = ston^{av,su}_{g,a,y,s,t} + ston^{av,sd}_{g,a,y,s,t} \\ \forall g \in \mathbb{STO}, a \in \mathbb{A}, y \in \mathbb{Y}, s \in \mathbb{S}, t \in \mathbb{T} \tag{A.70}$$

In order to reflect the discrete nature of the storage units that are part of the energy system, the following variables are restricted to be integer variables. In accordance with the Logical conditions of dispatchable units, this constrain can be also relaxed by defining the variables as continuous and reduce the computational time.

$$ston^{av,on}_{g,a,y,s,t}, ston^{av,su}_{g,a,y,s,t}, ston^{av,sd}_{g,a,y,s,t} \in \mathbb{Z}^{+} \\ \forall g \in \mathbb{STO}, a \in \mathbb{A}, y \in \mathbb{Y}, s \in \mathbb{S}, t \in \mathbb{T} \tag{A.71}$$

**Specific technological constraints for intermittent generation units**

Non-dispatchable technologies included are solar PV, solar heating, wind onshore and offshore, and hydro run of river.

Available electricity for generation is a function of the installed capacity and the time series in a given area

$$AE_{g,a,y,s,t} \geq p^{el}_{g,a,y,s,t} \\ \forall g \in \mathbb{GI}, g \in \mathbb{E}, a \in \mathbb{A}, y \in \mathbb{Y}, s \in \mathbb{S}, t \in \mathbb{T} \tag{A.72}$$

Likewise, available heat for generation is a function of the installed capacity and the time series in a given area

$$AH_{g,a,y,s,t} \geq p^{h}_{g,a,y,s,t} \\ \forall g \in \mathbb{GI}, g \in \mathbb{H}, a \in \mathbb{A}, y \in \mathbb{Y}, s \in \mathbb{S}, t \in \mathbb{T} \tag{A.73}$$

**Power transmission constraints**

Electricity exchange between neighboring regions is allowed but limited to the available transmission capacity. The available transmission capacity is calculated in each time step as the product of the Net Transfer Capacity and the availability of each connection in that time step.

$$TC_{r,r',y,s,t} \cdot TCR_{r,r',y,s,t} \geq x_{r,r',y,s,t} \\ \forall r \in \mathbb{R}, r' \in \mathbb{R}, y \in \mathbb{Y}, s \in \mathbb{S}, t \in \mathbb{T} \tag{A.74}$$

### A.2.2 Storage and planned maintenance optimisation formulation

The code is almost the same as the one in section A.2.1, with a few exceptions.

**Available units**

The first exception is related to the availability of the units, which is endogenised in this optimisation. Equations A.29, A.50, and A.51 are replaced with equations A.75, A.76, A.77, respectively. The equations calculating the availability factor (A.29 and A.52) are not used in this optimisation.

$$\frac{FC_{g,a,y}}{US_g^{gen}} - n_{g,a,y,s}^{nav,pm} \geq n_{g,a,y,s,t}^{av,on} \quad \forall g \in \mathbb{GD}, a \in \mathbb{A}, y \in \mathbb{Y}, s \in \mathbb{S}, t \in \mathbb{T} \tag{A.75}$$

$$\frac{EC_{g,a,y}}{US_g^{sto}} - n_{g,a,y,s}^{nav,pm} \geq n_{g,a,y,s,t}^{av,on} \quad \forall g \in \mathbb{STO}, a \in \mathbb{A}, y \in \mathbb{Y}, s \in \mathbb{S}, t \in \mathbb{T} \tag{A.76}$$

$$\frac{EC_{g,a,y}}{US_g^{sto}} - n_{g,a,y,s}^{nav,pm} \geq ston_{g,a,y,s,t}^{av,on} \quad \forall g \in \mathbb{STO}, a \in \mathbb{A}, y \in \mathbb{Y}, s \in \mathbb{S}, t \in \mathbb{T} \tag{A.77}$$

Additionally, the maximum amount of units on maintenance is limited by the total number of units

$$\frac{FC_{g,a,y}}{US_g^{gen}} \geq n_{g,a,y,s}^{nav,pm} \quad \forall g \in \mathbb{GD}, a \in \mathbb{A}, y \in \mathbb{Y}, s \in \mathbb{S}, t \in \mathbb{T} \tag{A.78}$$

$$\frac{EC_{g,a,y}}{US_g^{sto}} \geq n_{g,a,y,s}^{nav,pm} \quad \forall g \in \mathbb{STO}, a \in \mathbb{A}, y \in \mathbb{Y}, s \in \mathbb{S}, t \in \mathbb{T} \tag{A.79}$$

**Yearly maintenance requirement**

The equations A.80 and A.81 guarantee the hour of maintenance per unit is respected during the year:

$$\sum_{s \in \mathbb{S}} n_{g,a,y,s}^{nav,pm,su} \cdot SL_s = MMT_g \cdot \frac{FC_{g,a,y}}{US_g^{gen}} \quad \forall g \in \mathbb{GD}, a \in \mathbb{A}, y \in \mathbb{Y}, \tag{A.80}$$

$$\sum_{s \in \mathbb{S}} n_{g,a,y,s}^{nav,pm,su} \cdot SL_s = MMT_g \cdot \frac{EC_{g,a,y}}{US_g^{sto}} \quad \forall g \in \mathbb{STO}, a \in \mathbb{A}, y \in \mathbb{Y}, \tag{A.81}$$

**Uninterrupted maintenance**

Maintenance is considered to occur uninterrupted,in other words it can't be split into non-consecutive maintenance periods:

$$\sum_{s'=1}^{MMT_g} n^{nav,pm.su}_{g,a,y,s-s'} \leq n^{nav,pm}_{g,a,y,s} \quad \forall g \in \mathbb{GGG}, a \in \mathbb{A}, y \in \mathbb{Y}, s \in \mathbb{S} \tag{A.82}$$

**Logical conditions**

$$n^{nav,pm}_{g,a,y,s} - n^{av,pm}_{g,a,y,s-1} = n^{nav,pm,su}_{g,a,y,s} - n^{nav,pm,sd}_{g,a,y,s} \quad \forall g \in \mathbb{GGG}, a \in \mathbb{A}, y \in \mathbb{Y}, s \in \mathbb{S} \tag{A.83}$$

In order to reflect the discrete nature of the generation units that are part of the energy system, the following variables are restricted to be integer variables.

$$n^{nav,pm}_{g,a,y,s}, n^{nav,pm,su}_{g,a,y,s}, n^{nav,pm,sd}_{g,a,y,s} \in \mathbb{Z}^+ \quad \forall g \in \mathbb{GGG}, a \in \mathbb{A}, y \in \mathbb{Y}, s \in \mathbb{S} \tag{A.84}$$

### A.2.3 Stochastic outage simulations formulation

Using as input parameters the total capacity of a unit type in each area, the size of a single unit, the planned maintenance, and the probability of suffering an outage, Montecarlo simulations are performed for every timestep and unit in the system to simulate these outages. It is assumed that the outages last one hour.

$$n^{nav,so}_{g,a,y,s,t} = \sum_{i \in \mathbb{I}} so_{g,a,y,s,t,i} \quad \forall g \in \mathbb{GGG}, a \in \mathbb{A}, y \in \mathbb{Y}, s \in \mathbb{S}, t \in \mathbb{T} \tag{A.85}$$

$$so_{g,a,y,s,t,i} = \begin{cases} 1, & \text{if } x \leq SO_{g,i} \\ 0, & \text{otherwise} \end{cases} \quad \forall g \in \mathbb{GGG}, a \in \mathbb{A}, y \in \mathbb{Y}, s \in \mathbb{S}, t \in \mathbb{T}, i \in \mathbb{I}, x \sim U(0,1) \tag{A.86}$$

# Appendix B

# Mathematical model formulation of Intra-hour Market Model in OptiBal

## B.1 Methodology

The OptiBal model receives as input the hour ahead wind forecast simulations in temporal resolution of 5 minutes from CorRES and the hourly generation schedule from Balmorel. The main purpose of this model is to calculate the required adjustments from non VRE generators in order to counteract the imbalance occurred due to the mismatch of the DA wind dispatches and the new wind generation forecasts.

OptiBal is created as an add-on in the already existing Balmorel model. For that reason, the same methodology and structure of Balmorel was kept also in OptiBal. The temporal representation in OptiBal similarly to Balmorel consists of years $y \in \mathbb{Y}$ , which are disaggregated into seasons $s \in \mathbb{S}$ which are composed of time steps $t \in \mathbb{T}$. In contrast with the Day Ahead optimization, for the simulations of the Intra Hour balancing market the seasons represent hours and time steps represent 5 minute segments. The same three gradations (countries,regions,areas) for the geographical representation that are used in Balmorel are also used in OptiBal's algorithm. Again there are two types of generators participating in the Intra Hour market, the dispatchable generators and the non-dispatchable which obviously consist from the same technologies as in Day Ahead market. The algorithm used in OptiBal is identical with the one used in Balmorel with few exceptions which are described in B.2. The objective function, the constrains regarding the system operation and all the technological constrains of dispatchable and non-dispatchable generators are used as presented in chapter 5.

The methodology used to simulate the Intra Hour market can be split in two groups: Fixing Balancing Variables and the Balancing Market optimization.

The Intra Hour balancing market optimisation is performed on a hourly basis. The results are linked from hour to hour meaning that the results of the previous hour may limit the results in the next hour. This limitation is highly dependent on the flexibility of the different units. The flexibility of the units, endogenously from the model, determines

whether a unit is able to participate in the balancing market or not.

## B.2 Mathematical Formulation

### B.2.1 Fixing Balancing Variables

As mentioned, the main core of Balmorel's algorithm is kept in OptiBal, but with some differens with respect to the Day Ahead optimization (Balmorel).

The heat production schedule was fixed with Balmorel results in order to restrict the flexibility that the heat market could provide to the power market during balancing. The DA commitment of slow units was also fixed since these units are not able to participate in the balancing market. Slow units are considered those with start-up time, shut down time, or ramp-up time longer than 1 hour.

Furthermore, in contrary with the energy content levels of storage, for the case of storage units the storage price was used in the balopt optimization in order to capture their flexibility within an hour. Thus, the storage energy content was fixed only for the starting point of the year. These values come from the DA run.

**Hydro Energy Content**

$$\begin{gathered} hsl^{OptiBal}_{a,y,s} - hsl_{a,y,s} = 0 \\ \forall a \in \mathbb{A}, y \in \mathbb{Y}, s \in \mathbb{S}, s = 1 \end{gathered} \tag{B.1}$$

**Storage Energy Content**

$$\begin{gathered} soc^{OptiBal}_{g,a,y,s,t} - soc_{g,a,y,s,t} = 0 \\ \forall g \in \mathbb{STO}, a \in \mathbb{A}, y \in \mathbb{Y}, s = 1, t = 1 \end{gathered} \tag{B.2}$$

**Heat Production**

$$\begin{gathered} \sum_{t'} (p^{h,OptiBal}_{g,a,y,s,t'}) - p^{h}_{g,a,y,s,t} = 0 \\ \forall g \in \mathbb{HEAT}, a \in \mathbb{A}, y \in \mathbb{Y}, s \in \mathbb{S}, t \in \mathbb{T} \end{gathered} \tag{B.3}$$

**Slow Units**

$$\begin{gathered} p^{el,OptiBal}_{g,a,y,s,t} - p^{el}_{g,a,y,s,t} = 0 \\ \forall g \in \mathbb{SLOW}, a \in \mathbb{A}, y \in \mathbb{Y}, s \in \mathbb{S}, t \in \mathbb{T} \end{gathered} \tag{B.4}$$

### B.2.2 Balancing optimization

The OptiBal's optimization part is exactly the same with Balmorel meaning that the objective function, the system's and the technological constrains of dispatchable, storage and VRE units are identical as in A.2.1, A.2.1, A.2.1, A.2.1 and A.2.1 respectively.

DTU Wind Energy is a department of the Technical University of Denmark with a unique integration of research, education, innovation and public/private sector consulting in the field of wind energy. Our activities develop new opportunities and technology for the global and Danish exploitation of wind energy. Research focuses on key technical-scientific fields, which are central for the development, innovation and use of wind energy and provides the basis for advanced education at the education.

We have more than 240 staff members of which approximately 60 are PhD students. Research is conducted within nine research programmes organized into three main topics: Wind energy systems, Wind turbine technology and Basics for wind energy.

**Technical University of Denmark**
Department of Wind Energy
Frederiksborgvej 399
Building 118
4000 Roskilde
Denmark
Telephone 46 77 50 85

info@vindenergi.dtu.dk
www.vindenergi.dtu.dk